Project Title:	Transforming PV installations toward dispatchable, schedulable energy solutions
Project Period:	1/1/2012 – 4/30/2015
Submission Date:	06/15/2015
Recipient:	Advanced Energy Industries Inc.
Address:	1625 Sharp Point Drive Ft Collins Co. 80525
Website (if available)	http://www.advanced-energy.com/
Award Number:	DE-EE0005340
Project Team:	Portland General Electric Northern Plains Power Technologies Potomac Electric Power Co. Schweitzer Engineering Laboratories Inc.
Principal Investigator:	Mesa Scharf, Product Manager Phone: 541-323-4163 Email: mesa.scharf@aei.com
Business Contact:	Jordan Roerig**,** Engineering Program Manager Phone: 541-323-4781 Email: jordan.roerig@aei.com
HQ Tech Manager:	Guohui Yuan
HQ Project Officer:	Christine Bing
GO Grant Specialist:	Clay Pfrangle
GO Contracting Officer:	Clay Pfrangle

Executive Summary

The Advanced Energy led SEGIS-AC program represents an industry partnership driven collaborative effort to continue to lower the barriers to increasing penetration of PV on the grid while also lowering overall system cost consistent with the Department of Energy SunShot Initiative. The SEGIS-AC program follows the DOE sponsored three year SEGIS program, which had similar high level goals, but with a broader exploratory scope. In SEGIS-AC, the team carries forward a new communications based islanding detection technology developed during the SEGIS program. Advanced utility interactive controls are further developed, and a storage inverter system is developed focused on intermittency mitigation due to cloud induced transients. Communications based island detection coupled with advanced controls and a storage system are shown to improve utility distribution feeder performance and to enable increased solar PV penetration levels. By the conclusion of the program, multiple utilities and customers have expressed awareness and desire to make use of the technologies developed and demonstrated under this program. This factor has led the Advanced Energy led team to deem the program an overall success. The report following details the technologies developed and demonstrated, as well as industry engagement.

Table of Contents

Background

While no new IP was filed during the SEGIS-AC program, IP disclosed under the SEGIS program was used in communications based island detection implementation and demonstrations. During the program, various members of the team presented at a multitude of conferences describing the work done under this program and providing context for why it is important to the industry. This is especially apparent with regard to communications based island detection, a long term investment by the program team. While it is widely recognized in the industry that an alternate form of island detection is needed to enable high penetration of PV on the grid, it requires significant investment within the industry to drive visibility and ultimately adoption of a new technique. The technique was a focus of many conferences, industry working groups, and customer discussions. A partial list of conferences attended where the SEGIS-AC program work was highlighted includes:

1. Solar Power International
2. ISGT- Innovative Smart Grid Technologies conference (multiple years)
3. Intersolar
4. Various EUCI sponsored conferences
5. Western Protective Relaying Conference
6. IEEE Photovoltaic Specialists Conference
7. IEEE Sustainable Energy Technologies Conference
8. High Penetration Solar Forum
9. Bend Technology Forum

Publications include:

1. Field Testing of 3G Cellular and Wireless Serial Radio Communications for Smart Grid Applications
   Power and Energy Automation Conference, March, 2014
2. A Statistically-Based Method of Control of Distributed Photovoltaics Using Synchrophasors
   Power and Energy Society General Meeting, 2012 IEEE, 22-26 July, 2012, San Diego, CA
3. Synchrophasors for Island Detection
   Photovoltaic Specialists Conference (PVSC), 2012 38th IEEE, 3-8 June 2012, Austin, TX
4. Adaptive Control Strategies and Communications for Utility Integration of Photovoltaic Solar Sites, Power and Energy Automation Conference, March 2014, Spokane, WA

5. The Importance of Coordinated Control Systems in Solar Generation Plants, 1st Annual PAC World Americas Conference, September 23-25, 2014, Raleigh, NC

The bulk of the conference presentations as well as publications were focused specifically on driving awareness of the capabilities of PV inverters with advanced utility interactive controls, alternate island detection, and intermittency mitigation enabled by storage. Utility distribution and protection engineers understand power systems, but historically do not have broad awareness of the capabilities (and limitations) of PV inverters. The team spent time in conferences and industry working groups such as the IEEE1547 working group educating and advocating tools and techniques to enable increased amounts of PV on the grid. Advancements within the industry literature included a practical look at communications based islanding deployment using wireless technologies, looking at wide and local area control techniques for feeder optimization, and using synchrophasors (PMUs) on the distribution network for island detection.

Introduction

Advanced Energy's SEGIS-AC program was developed as a continuation of the highly successful SEGIS program administered by Sandia National Laboratories that ran over the time period of 2007 – 2011. In preparing for the SEGIS-AC program, Advanced Energy carefully reviewed industry state and progress, progress of internal R&D program, and the intended focus of SEGIS-AC. Conscious decisions were made regarding which initiatives to put on hold, which initiatives would be reduced to product, and which initiatives required further R&D or industry support. Based on these decisions and the focus of SEGIS-AC, Advanced Energy developed a SEGIS-AC program focused on further enabling utility integration of increasing penetration levels of PV.

Advanced Energy focused on three key areas to develop further under SEGIS-AC. The first area was focused on further development and demonstration of a new communications based island detection technique that was developed under the SEGIS program. As PV penetration levels continue to increase, traditional inverter based 'perturb and observe' island detection techniques breakdown and can create further grid instabilities. Alternatives are required, and the Advanced Energy SEGIS team developed a technique using synchrophasors at the distribution level of the utility network. The second area was focused on further development of advanced smart inverter functionality such as LVRT, volt/VAr, and droop controls. This area included strong involvement with industry standards working groups in conjunction with technical development and field testing. The final area was to develop a utility scale smart storage inverter focused specifically on intermittency mitigation from cloud induced transients. These three areas became the core Program Objectives as noted below.

Program Objectives

1. Develop, demonstrate and commercialize an island detection strategy that overcomes the power quality challenges associated with techniques commonly deployed today, performs reliably under high penetration scenarios, and will not false trip under normal grid events.
2. Develop, demonstrate, and commercialize a set of control algorithms for inverter VAr (volt-ampere reactive) and output power control which optimize feeder efficiency, reduce cycles on electromechanical voltage regulation equipment, and improve voltage stability throughout distribution feeders.
3. Develop, demonstrate and commercialize a ramp rate controller that is effective at reducing the photovoltaic (PV) output ramp rates caused by cloud induced transients at the distribution feeder level under a high penetration of PV.

Tasks Summary

To meet the program objectives, the team developed five program tasks. The first task was focused on infrastructure development and modeling, an initialization task in a sense to support the next three tasks, which correspond in order with the program objectives detailed above. The final task (four) was focused on project management and reporting. This task has been omitted from the report. Project management and reporting oriented deliverables are addressed throughout the document. Below is a detailed summary of the task deliverables and decision points.

Task 0: Feeder instrumentation, data gathering, and performance analysis

In Task 0 the team was focused on instrumenting a feeder on the West Coast (Canby-Butteville feeder in Portland General Electric (PGE) territory, and a feeder on the East Coast in PEPCO territory. The team was also focused on understanding and predicting feeder performance from a modeling perspective and looking at tradeoffs associated with PMU (phasor measurement units) installation configurations and communications alternatives. The most critical gate here was to have a clear plan with support from utility partners to instrument the feeders. Below is the subtask detail for this portion of the effort.

Year	Subtask	Detail
1	0.1	Phasor Measurement Unit Equipment Installation (PGE)
2	0.1	Data Collection and Analysis (PEPCO feeder)
2	0.2	Baseline Feeder Operations

Year	Subtask	Detail
2	0.3	Model Improvement and Prediction of Feeder Performance
3	0.1	Advantages of Dispersed PMU's for Field Validation
3	0.2	Data Rates and Communication Media

Task 1: Correlation Coefficient Based (CCB) Island Detection

In Task 1 the team was focused on further reducing the CCB island detection method to practice by more laboratory testing and refinement, field testing, as well as demonstration to drive awareness of the technique as a viable alternative. Milestones included field installation of PMU equipment to enable CCB island detection to run in parallel with existing solutions for island detection, 3rd party laboratory testing of the technique and further technical refinement to ensure the technique does not lead to false trips, but consistently identifies island cases within the IEEE1547 limits. Critical gates for this task included successful deployment of the CCB as well as third party laboratory demonstration and a written report documenting the findings. Below is the subtask detail for this portion of the effort.

Year	Subtask	Detail
1	1.1	Laboratory demonstration
1	1.2	Data analysis of feeder data to prove false trip immunity
1	1.3	Demonstration of added value of system-level PMU data
1	1.4	Development of a minimum-cost local PMU
2	1.1	3rd Party laboratory validation of CCB-Island detection algorithm
2	1.2	Economic model development for CCB-Island detection strategy
2	1.3	Demonstration on a live feeder
3	1.1	Economics of Solution
3	1.2	Qualification or Certification of CCB- island detection
3	1.3	Laboratory demonstrations of the technology
3	1.4	Islanding performance under loss of PMU data

Task 2: Advanced Inverter Functional Controls on Fielded Systems

In Task 2, the focus in close cooperation with industry working groups including the EPRI smart inverter working group, the IEEE1547a working group and CPUC was to develop and implement advanced inverter functional controls that would address real

world distribution feeder issues such as high cycle count on load tap changers due to high solar penetration. In addition to smart inverter functionality implementation, the team planned to focus on modeling specific feeders and look at the impacts of the developed autonomous controls, and finally to field the controls on select feeders and validate the model predictions. In addition, the team planned to address local vs. wide area control strategies, since the PMU equipment installed would afford opportunities to perform wide area optimizations (feeder level vs. POI level controls). In looking at these control strategies, the team would quantify impacts in terms of economics, ease of implementation, and improvement in overall voltage regulation. Critical gates for this task included performance of the optimization and reporting on a study of various feeders as well as fielding of the advanced controls on at least one live feeder. Below is the subtask detail for this portion of the effort.

Year	Subtask	Detail
1	2.1	Model development and validation to support control law design
1	2.2	Control developments in simulation
1	2.3	Hardware-in-the-loop, laboratory-scale validation of control laws
2	2.1	Validating inverter-based voltage support functions on selected distribution circuits
2	2.2	Volt/Var Optimization Using Wide Area Information
2	2.3	Energy Loss and Impact on Inverter Performance
2	2.4	Wide Area vs. Local Control Case Studies
2	2.5	PHIL Testing and validation of advanced inverter control functions
3	2.1	Field Testing Data Analysis
3	2.2	Field Demonstration of Advanced Inverter Capabilities
3	2.3	Determine Optimal Control Settings
3	2.4	Economic Analyses of Fielded Voltage Stabilization Functions
3	2.5	Evaluate Closed Loop Control of Voltage at a Remote Bus

Task 3: Ramp Rate Controller

In Task 3, the focus was in quantifying the benefits of applying storage to mitigate the effects of cloud induced transients. Because storage technology was generally still cost prohibitive for widespread adoption and deployment, the idea was to identify a utility scale application that used the minimum amount of storage possible while still providing

measurable benefit. The effort included better understanding the value and issues associated with power ramps, determining the economics associated with a ramp controller, and development of an inverter with ramp controls that could be used for model validation and field demonstration. This included installation of a completed battery system at a field demonstration site (originally planned to be on the Canby-Butteville feeder).

Year	Subtask	Detail
1	3.1	Understanding the value of ramp rate control to power marketers.
1	3.2	Optimal sizing of the energy storage medium for the ramp-rate control application
2	3.1	Laboratory testing of the ramp rate controller
2	3.2	State of Charge Algorithm
2	3.3	Equipment installation
2	3.4	Factory Acceptance Test using Scaled System
2	3.5	Validation Plan for Battery Economics
3	3.1	Final Installation of the Battery Storage Solution
3	3.2	Ramp Rate Controller Demonstrations
3	3.3	Peak Shifting Demonstration
3	3.4	Pricing Signal Demonstration

Project Results and Discussion

This section is broken into five main areas: The first area discusses the development and evolution of the partnerships that enabled the progress envisioned by this SEGIS-AC program team. The last four areas cover SEGIS-AC program tasks 0-3 in order. This section focuses heavily on development, results, analysis of the results and briefly on overall status at the conclusion of the program.

Partner selection, development, and evolution

At the outset of the program, the team identified the following partners to participate in the program, encouraging industry collaboration, progress, and visibility to the work undertaken over the three year program period. Below is a brief overview of each partner and their expected role.

1. PGE (Portland General Electric): Northwest utility covering primarily the Portland, OR metro area. Valuable partner in both the SEGIS (earlier DOE program administered by Sandia National Laboratories) and SEGIS-

AC programs. PGE developed a leading distributed energy management platform called GenOnSys that manages dispatchable standby generation (primarily diesel gensets throughout the metro area) and makes the generation available during times when extra generation is needed. The solar resources were also integrated into this platform. Multiple studies and demonstrations were performed throughout the SEGIS and SEGIS-AC programs on PGE feeders.

2. NPPT (Northern Plains Power Technologies): NPPT led by Dr. Mike Ropp is a consulting company in South Dakota. Mike is a known expert in the field of power systems and islanding detection. NPPT's role included modeling, development and refinement of the CCB, model validation.
3. PEPCO (Potomac Electric Power Company): PEPCO is a utility in the Northeast with many long rural feeders and relatively high penetration of PV due to favorable PV installation economic incentives in their region. PEPCO's role included providing feeder parameters for modeling as well as identification of candidate feeders for field monitoring and demonstration of synchrophasor based island detection (CCB) and smart inverter functionality.
4. SEL (Schweitzer Engineering Laboratories): SEL is a leading utility automation, protection and control company based in Pullman, WA. SEL's role included providing hardware and software tools and support enabling deployment of the CCB and system level controls for the BIS. They also bring credibility to utility protection conversations and ultimately acceptance of new technology.

Over the course of the program, a number of developments occurred that affected the partnerships developed at the outset of the program. NPPT proved an invaluable partner throughout the program. NPPT made valuable contributions on nearly every task with special focus on modelling and CCB algorithm development and validation.

PEPCO represented our East coast utility partner and has had significant field challenges on their network, holding many older feeders with long rural segments and PV systems installed in remote areas where PV has significant impacts on feeder performance and operation. During the program (and when they were approached as a partner), PEPCO was extremely busy working through the tactics of existing interconnects and existing programs. Over time, this coupled with the geography of managing a long distance partnership and challenges identified early on associated with feeder instrumentation and data backhaul led a reduction in scope of the PEPCO partnership. PEPCO supported modeling activities enabling analysis of the benefits of smart inverter operation of various feeders on their network. However, ultimately instrumenting an East coast feeder on PEPCO territory became unfeasible.

Portland General Electric was a strong partner at the outset of the program, energized from the earlier DOE SEGIS program administered by Sandia National Laboratories. The management team at PGE also held a progressive mindset in spite of the fact that the economics for commercial and utility scale solar in the State of Oregon were not all that favorable. Significant progress was made during the first two years of the program with PGE, getting an entire feeder instrumented and modelled, multiple discussions with utility engineers, and demonstrating VAR control at the Baldock 1.4MW solar site. Later in the program however, management changes, concerns related to long term responsibility for the BIS, and the fact that storage for transient mitigation was not required at Baldock from a business perspective led to stalls in the partnership and ultimately an inability to site the 300kW BIS at the site. While system level simulations were performed and validated with feeder data, an actual field test with end to end model validation was not able to be completed during the SEGIS-AC program.

SEL, a leader in utility protection, instrumentation, automation and control was a strong partner during the Sandia administered SEGIS program and this successful partnership was carried forward in SEGIS-AC. SEL was instrumental in supporting development of the CCB early and assisting in identifying various issues surrounding reduction to practice. SEL also provided all of the phasor measurement equipment for the Canby-Butteville feeder instrumentation as well as laboratory instrumentation and automation equipment for all of the various tests and tasks performed throughout the program including instrumentation at NPPT laboratories, the Sandia DETL (Distributed Energy Testing Laboratory), and Advanced Energy laboratories.

Task 0: Feeder instrumentation, data gathering, and performance analysis

In this task, the team instrumented a Portland General Electric distribution circuit with phasor measurement units (PMUs). This feeder also hosts a PV plant using Advanced Energy inverters (Baldock). Approximately three years' worth of data was collected, and these data were used for a number of different analyses, including;

- Ramp rate characterization of the PV plant
- Characterizing the PV plant impact on feeder voltages and on voltage regulators
- Validation of detailed transient circuit models of the feeder and PV plant
- Testing of the CCB islanding detection method (described below)

Description of the circuit

An EMTP-RV block diagram of the selected distribution circuit is shown in Figure 1. This circuit selected serves primarily agricultural load, with some light industrial load and also a small airport. The feeder is a four-wire overhead circuit with a multigrounded neutral, operated at 12.47 kV. The feeder has two line regulators, as shown in Figure 1, but no capacitors.

Figure 1 shows that the feeder has one main trunk line extending from the substation to a branch point, and three branches, North, West and South, leave that branch point. About 50% of the feeder load is on the West branch, and the 1.4 MWAC PV plant is at the distal end of the West branch, approximately 12 km from the substation. The West branch also serves an unusual large-motor load that includes multiple induction motors in the hundreds of horsepower. These motors are connected to variable speed drives, but because of the way they are used they present a highly dynamic load to the feeder.

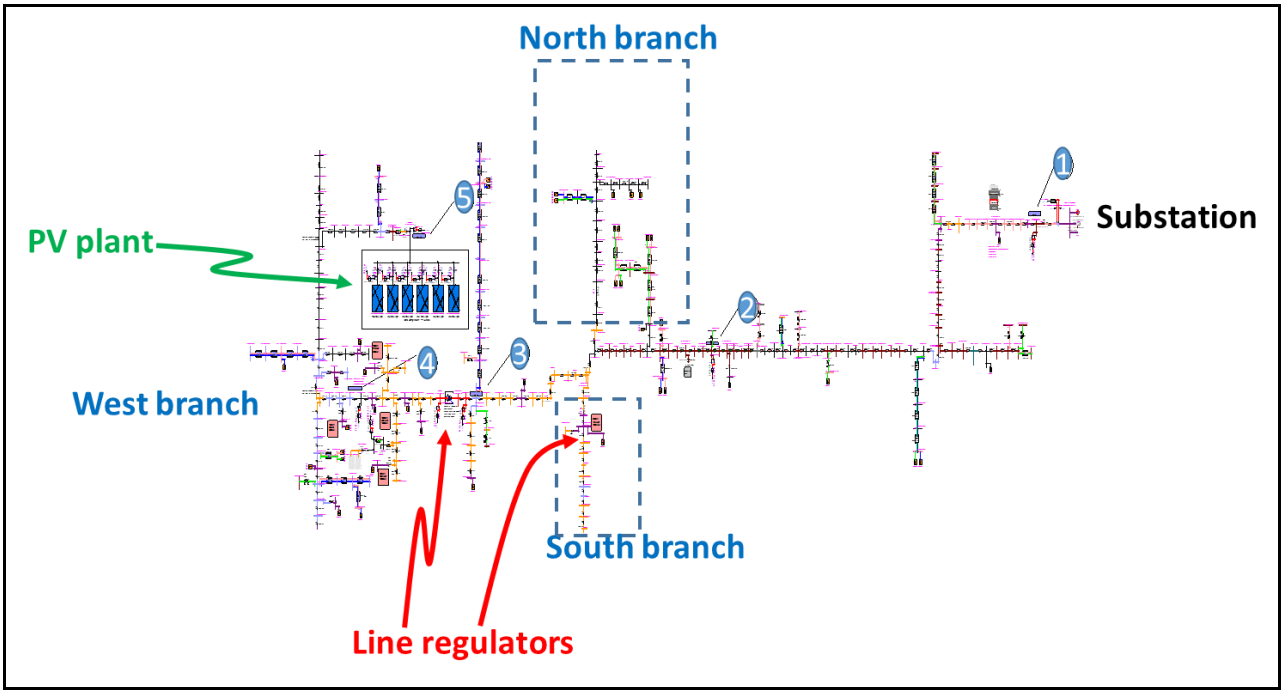

Figure 1. EMTP-RV model of the test circuit.

Circuit instrumentation

The numbers in the blue ovals in Figure 1 show the locations of the five phasor measurement units (PMUs) installed on this feeder. PMU1 is just outside the substation. PMU2 is just upstream from the branch point. PMUs 3 and 4 are just upstream and downstream (respectively) of the line regulator on the West branch. PMU5 is on the LV side of the PV plant GSU transformer. Figure 2 shows the communications architecture used to collect the PMU data. The PMUs communicate via 900 MHz radio to a data Phasor Data Concentrator (PDC) located at the PV plant (next to PMU5).

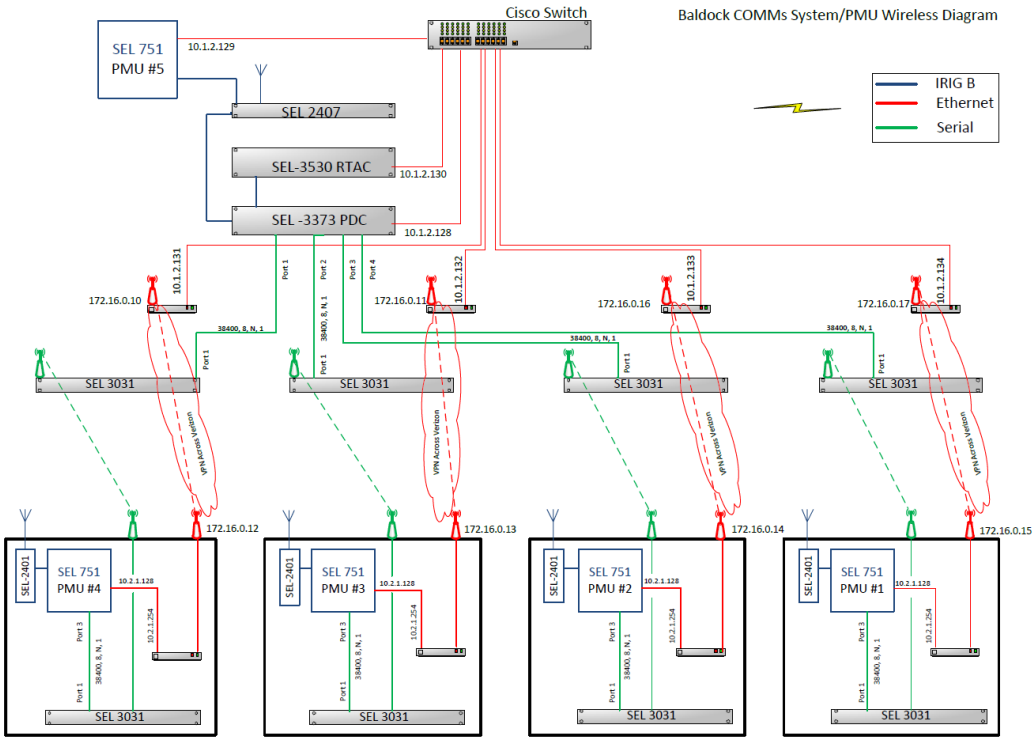

Figure 2. Block diagram of the communication architecture between the circuit PMUs.

Circuit modeling

The models of this circuit include detailed models of the PV inverters, the line regulators and their controls, and the measurements and processing done by the PMUs, and it also includes a behavioral model of the motors and their VSDs ("behavioral" meaning that the model was derived from empirical measurements and was set up so that under the same test conditions the model results match the experimental results). Figure 3 shows the motor + VSD behavioral model in EMTP-RV. Figure 4 shows the modeled startup current for one of the motor + VSD units.

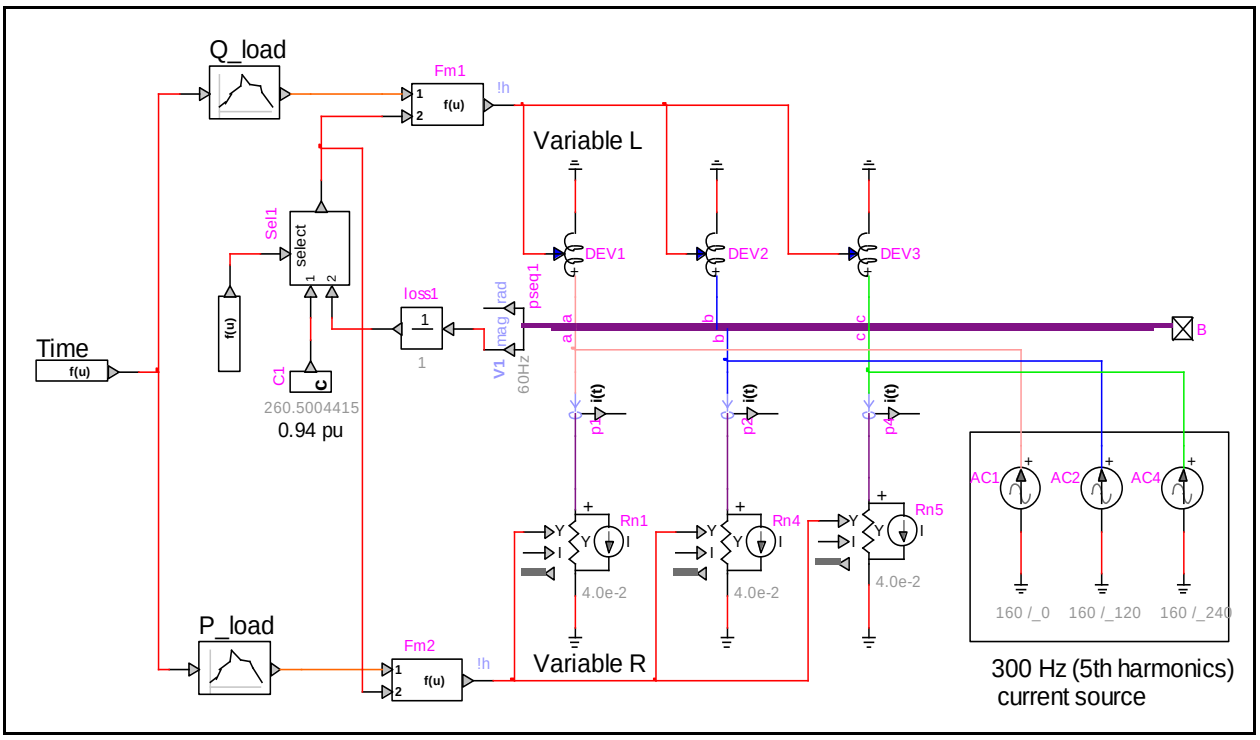

Figure 3. EMTP-RV model of the motor load and VSD soft-starter.

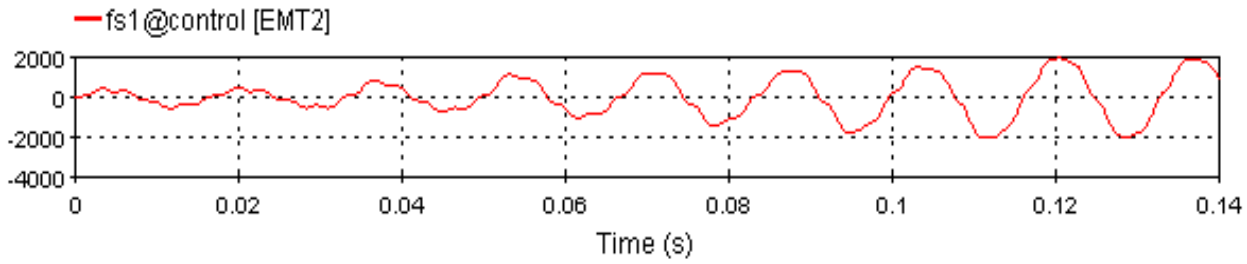

Figure 4. Current drawn by the modeled motor + VSD soft starter during startup.

The PV inverters' anti-islanding, MPPT, current regulating, and protection functions are all included in the model. The model also includes a volt-VAr function, programmed to follow the characteristic curve shown in Figure 5. The parameters V1-V4 are user-adjustable, and default or starting values are shown in the figure.

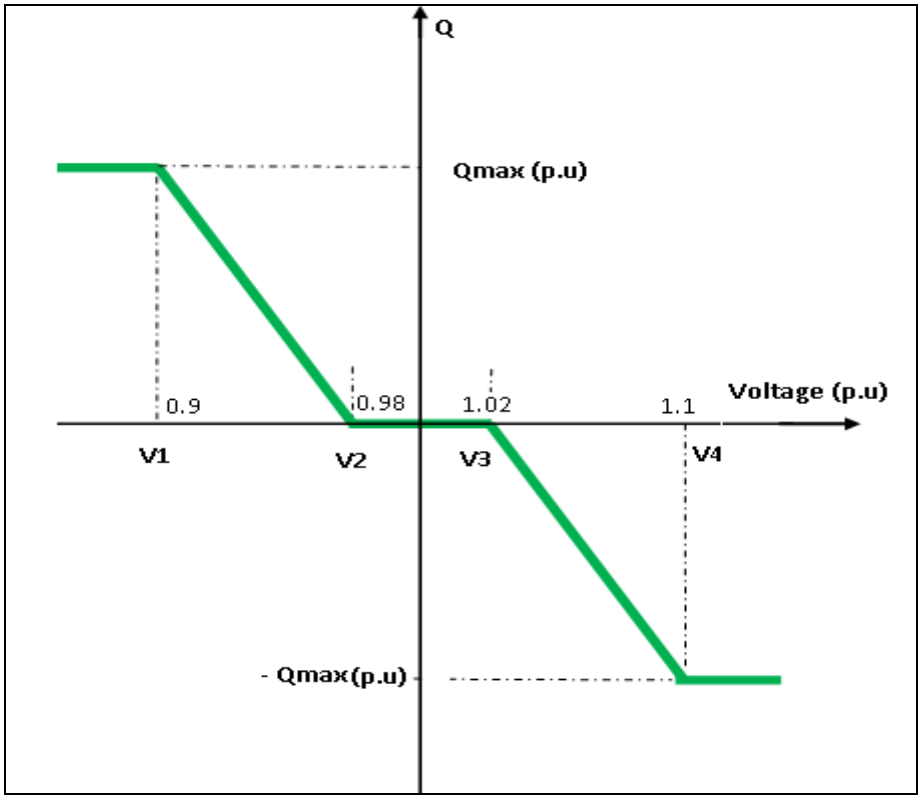

Figure 5. Volt-VAr curve used in the PV plant model. The voltages V1-V4 are adjustable; the values in the figure are the defaults.

Later in the project, a MATLAB/Simulink model of this same feeder was developed from the utility-provided data and the EMTP-RV model. The additional circuit model was developed because there were certain inverter functions that were modeled in a higher degree of detail in MATLAB/Simulink.

Circuit model validation

The measured data collected from the feeder described above were used to validate and improve the circuit models. Three separate aspects of the model were validated: the feeder impedances, the load models, and the voltage regulator models. The feeder impedances were initially validated using fault current calculations from the utility. With the availability of much more detailed data from the PMUs, "snapshot" validation of the impedances from specific moments in time became possible. A "snapshot" validation involves setting the source voltage, all of the feeder loads, and the PV plant output in the model according to the loading indicated by the PMU data. These can be thought of as the model inputs. Then, a simulation is run to check whether the model predicts the correct voltage (magnitude and phase) at each PMU bus. These voltages and phases are the outputs. If they match, this means the feeder segment impedances and the steady-state loading distribution in the model must be correct. "Snapshot" calculations

were run for several time instants from the PMU data, and a set of representative examples is shown in Table 1. The model-predicted voltages match the measured ones extremely well, indicating that the model does represent the feeder faithfully at least in the steady-state sense. The matching at PMU 5 (the PV plant PMU) is not quite as good; these data show an approximately constant 9^{o} phase error between the modeled and measured values (highlighted in red in Table 1). At this time, this is believed to be due to a discrepancy in the transformer impedance, and possibly secondarily due to impedances in the PV plant conductors. This can be corrected, but the error is not large enough to warrant concern.

Table 1. "Snapshot" validation of feeder impedances.

Date and Time (GMT)		PF substation	PMU 4		PMU 3	PMU2	PMU1	PMU5
			V (pu)	I (Amps)	V (pu)	V (pu)	V (pu)	V (pu)
April 09, 2013 00:16:00	Field	0.861	1.006 ∟109.1	9.4842 ∟78.69	1.006 ∟109.1945	1.011 ∟109.444	1.012 ∟109.962	1.011 ∟118.50
	Simulated	0.844	1.006 ∟109.09	9.27 ∟76.64	1.005 ∟109.054	1.005 ∟109.07	1.005 ∟109.108	1.007 ∟109.48
April 10, 2013 22:42:00	Field	0.87235	1.002 ∟117.68	10.54 ∟90	1.018 ∟117.766	1.002 ∟117.99	1.023 ∟118.981	1.007 ∟127.02
	Simulated	0.863	1.0024 ∟117.67	11.09 ∟87.44	1.001 ∟117.62	1.0011 ∟117.62	1.001 ∟117.66	1.002 ∟117.9
April 10, 2013 20:52:00	Field	-0.426	1.006 ∟59.383	11.177 ∟-56.31	1.007 ∟59.4675	1.0134 ∟59.8897	1.0188 ∟60.9426	1.0146 ∟69.42
	Simulated	-0.43	1.006 ∟59.38	12.82 ∟-56.07	1.005 ∟59.43	1.005 ∟59.511	1.005 ∟59.58	1.0116 ∟60.46
April 10, 2013 19:35:00	Field	-0.948	1.005 ∟118.01	44.941 ∟-44.16	1.005 ∟118.017	1.01 ∟118.264	1.006 ∟118.76	1.0186 ∟129.59
	Simulated	-0.953	1.005 ∟118	43.77 ∟-44.4	1.005 ∟118.29	1.0057 ∟118.52	1.007 ∟118.69	1.0207 ∟120.8

The availability of the measured data also enabled a further refinement of the model. It is common practice to adjust the loading level on the feeder using a pair of multipliers that adjust either the real and reactive loading (P and Q), or the total kVA loading and the power factor. Either way, this pair of multipliers is usually applied to all of the loads along the entire feeder because normally measured loading or power factor data are available only at the substation. The presence of the five PMUs on this feeder changes that, and now the loading in the MATLAB/Simulink model of the Canby-Butteville feeder can be adjusted on a section-by-section basis with the section boundaries being the PMU locations. The newly-refined model has multipliers for the P and Q between PMUs 1 and 2, another set of multipliers for the P and Q between PMUs 2 and 3, and so forth.

Modeling of other circuits

Four Pepco distribution circuits were also modeled as part of this work, but as noted above these circuits were not instrumented with PMUs. These additional circuits were all 12.47 kV, four-wire circuits hosting PV plants using Advanced Energy inverters. They included both strong (low source impedance) and weak (high source impedance) feeders. All of these Pepco feeders have power factor correction capacitors. Detailed time-domain transient models of these circuits similar to the one described above were created in EMTP-RV and/or MATLAB/Simulink. These models were used to quantify the expected benefits of PV volt-VAr control on the operation of utility voltage regulation equipment.

Circuit characterization via modeling—impact of volt-VAr controls on tap changers

The models were used to predict the potential impact of PV plant volt-VAr controls on the number of tap-change operations of the line regulators. Figure 6 shows one example, derived from simulations of the circuit shown in Figure 1 and with the volt-VAr curve shape shown in Figure 5. In these simulations, a cloud passes over the PV plant starting at t = 40 s, and the PV plant output power steadily drops to 20% of its clear-sky value. The cloud shadow moves off of the PV array starting at t = 70 s, and the PV output climbs back to 100%. Figure 6 shows the impact of this cloud shadow passage on the tap position of the West branch line regulator, for three different sets of volt-VAr curve settings. The dark blue curve is with the volt-VAr controls turned off (PV at unity power factor), the green curve is with the volt-VAr controls on with the default settings, and in the red curve the “deadband” between V2 and V3 in Figure 5 has essentially been reduced to zero. The results indicate that inclusion of volt-VAr controls does diminish the number of tap changer operations incurred by PV variability by four tap changes in this case (from eight changes to four), but does not eliminate them entirely.

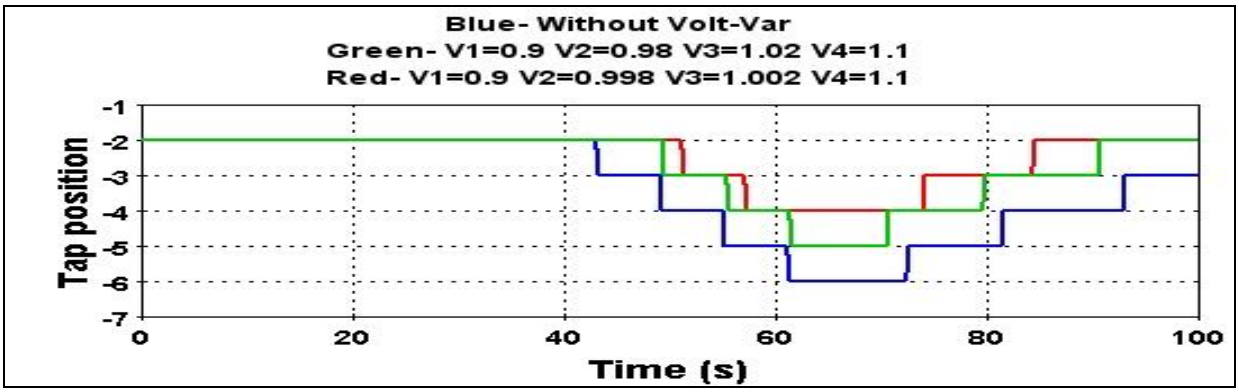

Figure 6. Tap position of the West branch line regulator, as a function of PV plant volt-VAr curve settings, during a simulated cloud shadow passage.

Simulations were also run to gain insights into the potential impact of PV volt-VAr controls on tap changer operations that were initiated by load variability, instead of PV plant output variability. Figure 7 shows an example result from these simulations. The large motor load is started at t = 25 s, and turned off at t = 75 s. Here the red curve is the baseline case with the PV operating at unity power factor and without any volt-VAr controls, and the other curves are results from simulations using varying widths of deadband in the volt-VAr curve. The volt-VAr controls have a slightly larger impact in this case, reducing the total number of tap changes from ten to four when the deadband is narrowest. This is expected, because although the motor load is considerably smaller than the PV plant, its startup current draw is far from unity power factor. The PV plant's ability to supply the needed VArs from a source more proximal to the load than the utility source has a significant beneficial impact on the feeder voltage profile and on the demand placed on the line regulator.

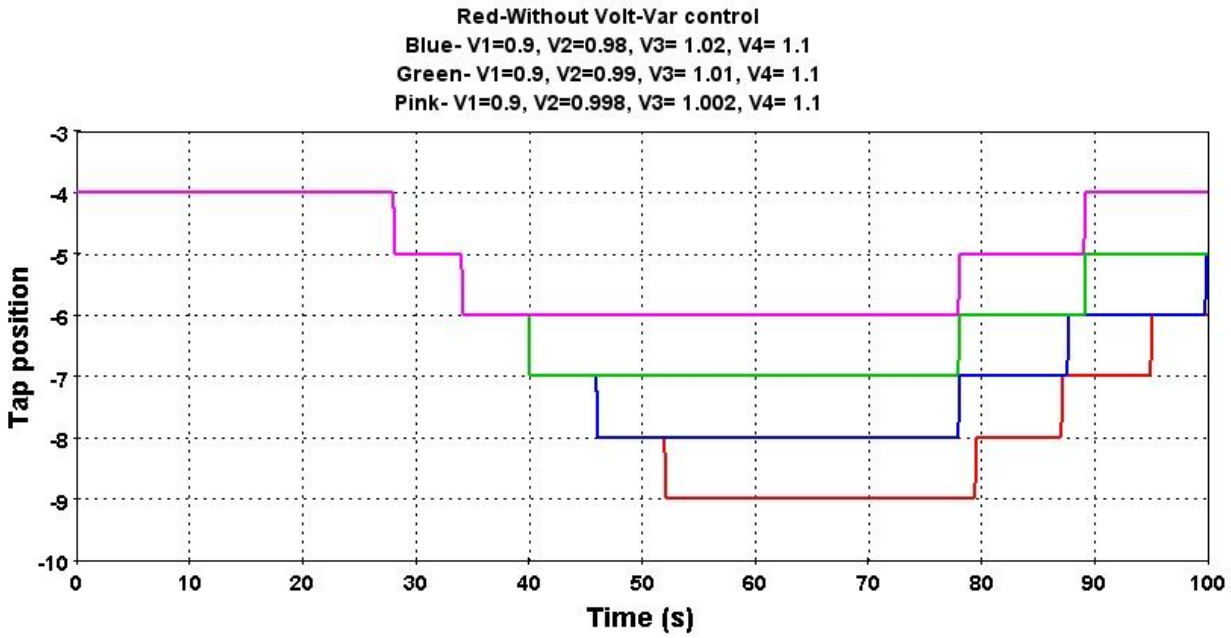

Figure 7. Tap position of the West branch regulator, as a function of PV plant volt-VAr curve settings, during a startup and shutdown of the large motor load.

Simulation results from the Pepco feeders showed that the ability of PV volt-VAr controls to impact circuit voltage profiles or tap changer operations is highly variable from one circuit to another. The case shown above is one of the cases that showed high benefit, but one of the Pepco circuits showed almost no impact from PV volt-VAr control at all. There are several variables that affect the benefit obtained from volt-VAr controls:

- The X/R ratio of the circuit. Fundamental circuit theory teaches that if the equivalent source impedance as seen from the PV inverter terminals has a low X/R ratio, the ability to mitigate PV real power output variability using VArs is diminished. In those cases in which the X/R ratio is less than unity, which can happen with long, older, or rural feeders, and also for residential PV where the service drop impedance must be included, then volt/VAr controls are ineffective in mitigating the impact of PV output variability on feeder voltage; one must control voltage using real power, and in general this requires the inclusion of energy storage, using either ramp rate or power smoothing controls.

- The location of the PV on the feeder. In particular, if the PV is located close to the substation and the utility source impedance as viewed from the substation secondary is relatively low, then VArs sourced from the PV plant are being sourced from essentially the same location as VArs sourced from the utility, and the PV-supplied VArs must flow through all of the same circuit impedances as

the utility-supplied VArs. As a result, the PV-supplied VArs cause very little change in the operation of downstream utility voltage regulation equipment.

- The configuration of the feeder circuit. Consider a situation of a feeder with two main branches, a PV plant on one of the two branches, and a voltage regulator located upstream from the branch point on the feeder. In this situation, the PV's volt-VAr controls may have little or no effect on voltages on the other circuit branch. In addition, if the PV is exporting it could actually cause the regulator to respond to conditions that do not exist on the branch without PV, leading to voltage excursions beyond allowed ranges on the branch without PV.

Table 2 summarizes the results of the feeder benefit testing on all five simulated feeders. In each case, tests were run to determine the benefit of volt-VAr controls on mitigating voltage variations caused by a) cloud shadow passages, and b) a major switching event (in the case of the instrumented feeder, sudden starting of the motor load between PMUs 3 and 4; on the other feeders, simultaneous tripping of all of the feeder capacitors). Three categories of benefits were examined:

- Do the volt-VAr controls reduce the number of tap changer operations of electromechanical voltage regulators during cloud shadow passages or load switching events?
- Do the volt-VAr controls mitigate the voltage sag that occurs during a cloud shadow passage or load switching event?
- Do the volt-VAr controls reduce feeder losses, and thereby reduce costs?

In each column, the Yes/No indicates whether the specific test in question was done on that feeder, and the numerical value following the Yes/No indicates the level of benefit obtained through the use of volt-VAr controls. In all of the results in Table 2, V2 = 0.998 and V3 = 1.002. For those results displaying the club (♣) symbol, V1 = 0.99; otherwise, V1 = 0.9. The feeder that shows "N/A" in the tap changer column had no line regulators outside of the substation.

Table 2. Summary of the potential benefits of PV plant volt-VAr control on five simulated feeders.

Feeder	Potential Benefit test					
	Tap reduction test? / Reduction in number of tap changes		Voltage sag/swell reduction test? / Approx % reduction in sag depth		Loss reduction test ?/ Approx % reduction in feeder losses (peak loading)	
	Cloud case	Switching case	Cloud case	Switching case	Cloud case	Switching case
CANBY-BUTTEVILLE	Yes, 2	Yes,3	Yes, 1.2	Yes, 3.2	Yes, 0.05	Yes, 0.1
NJ1112	Yes,0	Yes, 1	Yes, 0.7	Yes, 2.2	Yes,0.33	Yes, 0.61
NJ0813	Yes, 1♣	Yes, 1♣	Yes, 0.91	Yes, 2	Yes, 0	Yes, 0.05
NJ0428	NA	NA	Yes, 0.6	Yes, 0.2	Yes,0	No
IceRink 15123	Yes, 1♣	Yes, 1♣	Yes, 0.46	Yes, 2	Yes, 0	Yes, 0.07

♣ Using the "aggressive" V1 setting.

Task 1: Correlation Coefficient Based (CCB) Island Detection

The Correlation Coefficient Based (CCB) method of detecting islands via synchrophasor data was first conceived and developed by the Advanced Energy team during its original SEGIS grant. The CCB is important because it, along with other synchrophasor-based islanding detection means, has the potential to eliminate islanding as a barrier to deployment of distributed energy resources (DERs). In theory, the CCB can detect island formation for any combination of DERs, with or without smart inverter functions, in strong or weak grids. In SEGIS-AC, the ideas have been further refined, and a great deal of additional testing has been performed. Due to the support of the DoE through SEGIS-AC, the CCB is now ready for large-scale field trials, and this is considered a major success of the program.

Synchrophasor-based islanding detection is implemented using a configuration like that shown in Figure 8. A reference PMU is placed at some point upstream from the DER, outside of the island to be detected. This PMU's synchrophasor data are broadcast to all DERs within its service area (a microwave link is shown here). There is a second

PMU, the local PMU, collocated with the DER. At the DER location, the PMU data from the reference and local PMUs are processed and used to determine whether the island is still connected to the larger system. The CCB represents one such type of processing.

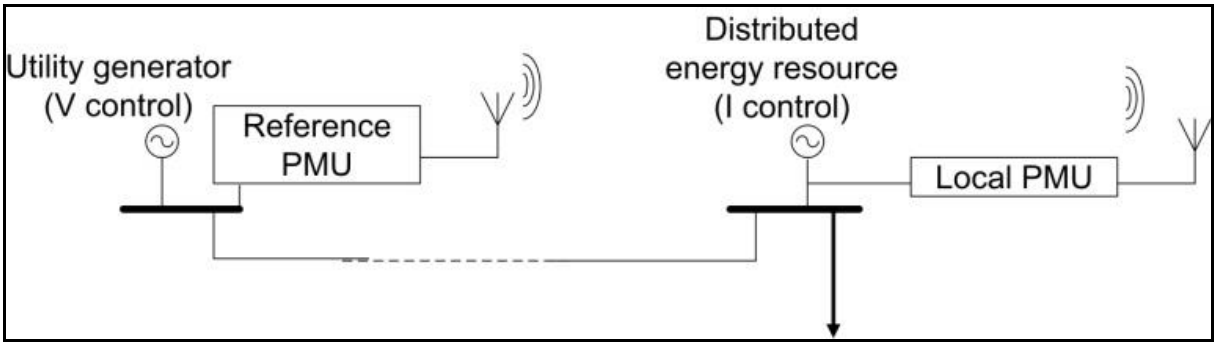

Figure 8. Schematic representation of an implementation of a synchrophasor-based islanding detection method.

During this work, a second synchrophasor-based islanding detection algorithm was tested: the Integral of Frequency Error (IFE). This method was first conceived in 1998 by a member of the Advanced Energy SEGIS-AC team[1], but the method was never fully vetted, reduced to practice, or formally published because at that time the needed reference frequency measurement was not readily available. The IFE of that time compared instantaneous local frequency measurements against long-term windowed average local frequency measurements, and the results were unimpressive. However, synchrophasors have made the reference frequency measurement available, and the Advanced Energy SEGIS-AC team added the IFE to the testing regimen to see how it might fit into the suite of synchrophasor-based island detection tools.

The islanding detection effectiveness of the CCB was demonstrated in the first SEGIS project by this team[2]. In SEGIS-AC, the CCB/IFE work was designed to carry this progress farther forward and move synchrophasor-based island detection toward readiness for full field deployment. To that end, the CCB/IFE work performed as part of SEGIS-AC fell into three broad categories:

- Testing of false trip immunity using field data
- Formal laboratory testing of its island detection effectiveness

[1] Dr. Michael Ropp first experimented with the IFE as part of his doctoral thesis work at Georgia Tech in 1998.
[2] See, for example, M. Ropp, D. Joshi, M. Mills-Price, S. Hummel, C. Steeprow, M. Osborn, K. Ravikumar, G. Zweigle, "A statistically-based method of control of distributed photovoltaics using synchrophasors", IEEE Power and Energy Society General Meeting, July 2012, 7 pgs.

- Analysis of the implementation cost of the CCB and its impact on PV costs

False trip immunity testing

The CCB + IFE were tested for immunity to false trips using field data collected over approximately three years on the PMU-instrumented northwestern US feeder. The CCB and IFE algorithms used are identical to those used in actual fielded hardware. Initial results showed a need for improvement; the CCB and IFE showed an average of one daylight-hours false trip per every four days' worth of simulation data. Some improvements were implemented, and it is believed that this rate has been reduced to less than one daylight-hours false trip per fifteen days' worth of operation, and further improvements are possible.

Figure 9 shows a representative example of the results. The top plot shows the frequencies measured by PMUs 4 and 5, the middle plot shows the correlation between the frequencies, and the bottom plot shows the IFE. During the time period shown, there are no islands and no significant grid events. The frequency measurements are clean, the correlation remains very close to 1, and the IFE remains close to zero, which is the desired result. Over 90% of the data sets tested fell into this category (no grid events and no false trips).

Figure 10 shows results from a 24-hour period early in the data set in which a very noisy load, the large motor load between PMUs 3 and 4, was operating. The irregular demand of this load leads to jitter in the measured voltage phases, and that phase jitter translates into noise in the PMUs' frequency measurements that adversely impacts the performance of the CCB and IFE. In Figure 10, the top plot is the measured frequency reported by PMUs 4 and 5, the second plot shows the difference between the PMU 4 and 5 frequencies, the third plot shows the correlation of the frequencies, and the bottom plot shows the IFE. Over this 24-hour period, there are two moments at which the correlation dropped below the default trip threshold value of 0.8, and both of these would have been false trips. The lowest correlation seen was 0.76. In this case the IFE did not falsely trip, but elsewhere in the data set there were cases where the CCB did not false trip and the IFE did. As a result of this testing, the CCB threshold was subsequently reduced to 0.7, and the IFE gain value was reduced.

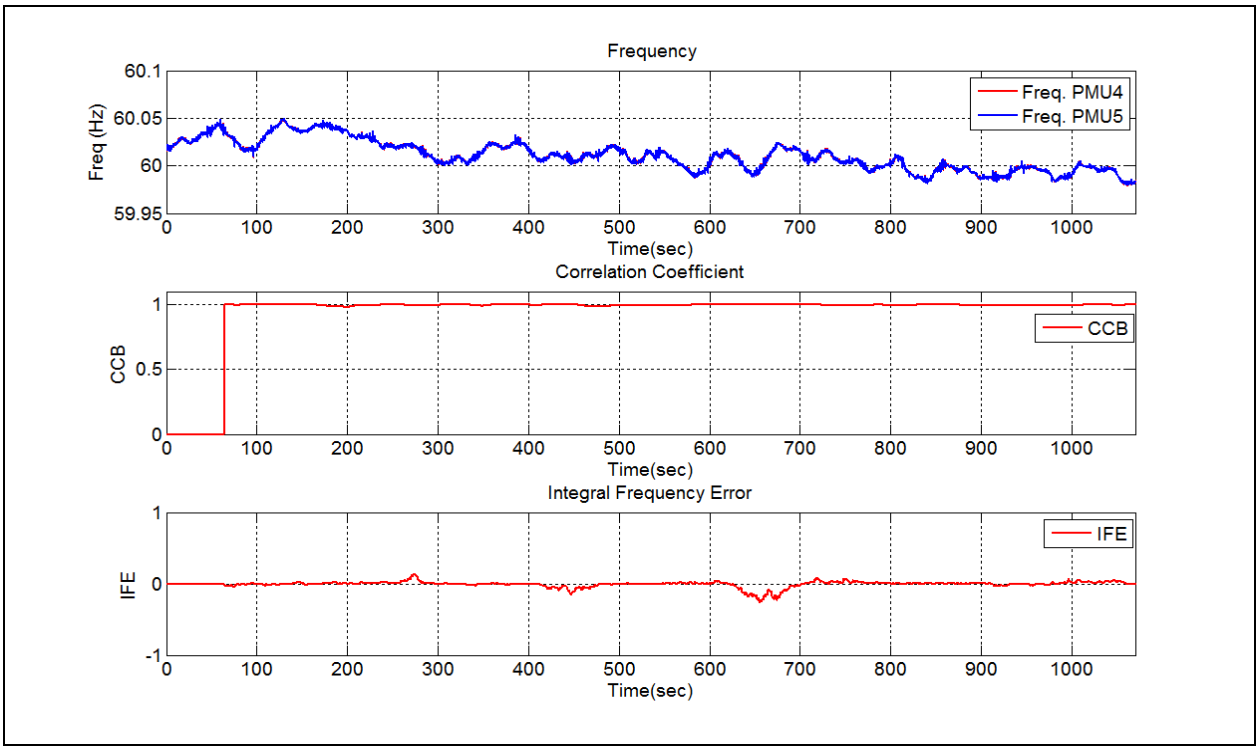

Figure 9. A representative example of a day's worth (Nov 16, 2013) of measured feeder data post-processed with the CCB and IFE algorithms.

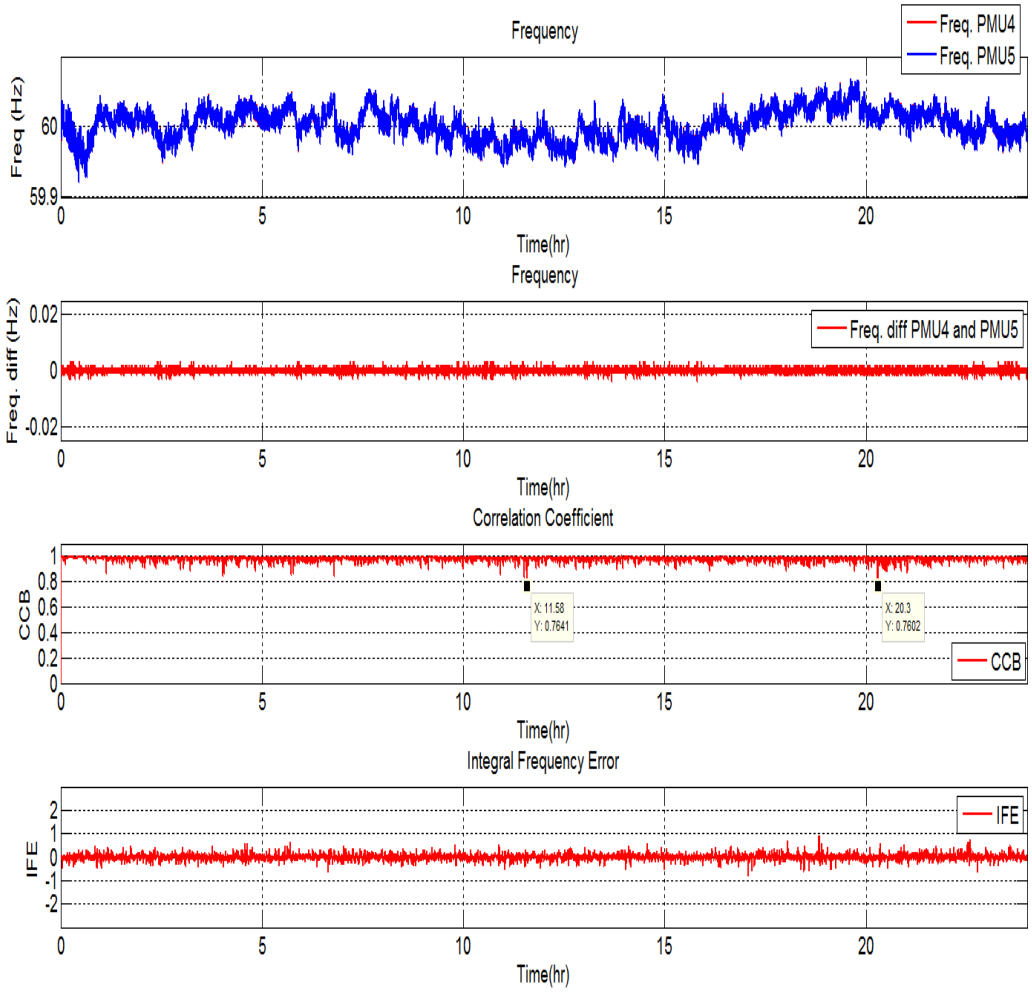

Figure 10. Example of a "noisy day" in which either the CCB or IFE breaches its trip threshold when no island was present (in this case, the CCB does this twice over the 24-hour period shown).

During the three-year data collection period, there were a total of four significant frequency events seen on the system. At least two were associated with the tripping of a large wind farm elsewhere on the system; for the other two events, the specific cause was never conclusively determined. Figure 11 shows the data and CCB + IFE performance during one of these events. The top plot shows the frequencies at PMUs 4 and 5, and the bottom plot shows both the correlation and IFE. Throughout the loss of generation event, the CCB remains very close to 1, which is as expected. There is a momentary surge in the IFE just as the event starts, but the IFE does not reach its trip threshold (±1), so the CCB + IFE successfully rode through this event, as desired.

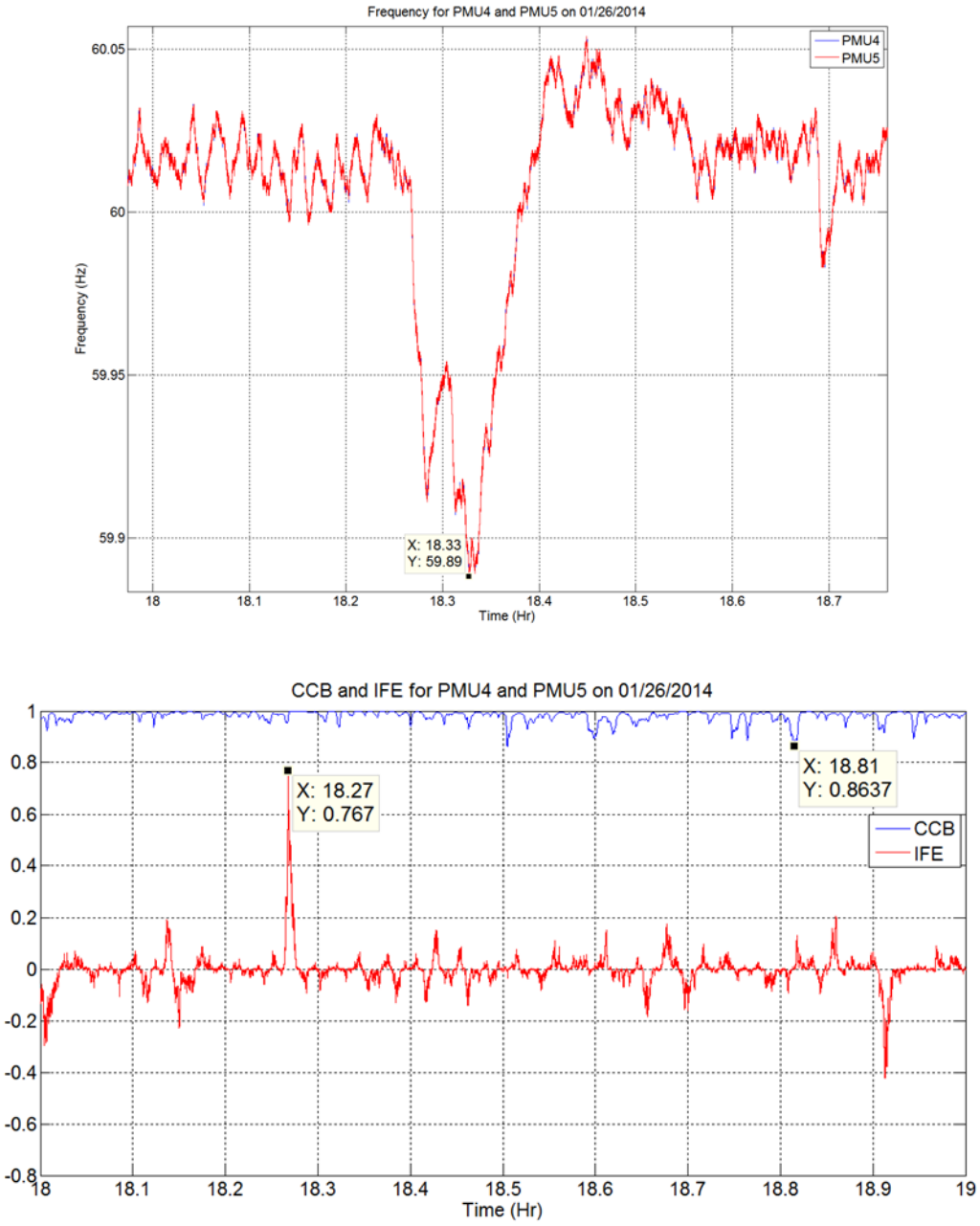

Figure 11. Example of a significant frequency event on the system, triggered by the loss of a large wind farm, and the corresponding CCB + IFE results.

Figure 12 shows another system-level frequency event, again triggered by the loss of a large wind farm elsewhere on the system. Over the span of a few seconds, the system frequency declines by 220 mHz. Figure 13 shows the correlation between the frequencies at PMUs 1 and 4 (blue trace) and also between the PMU 1 and 5 frequencies (red trace). Recall that PMU 4 is on the MV side of the PV plant GSU transformer and PMU 5 is on the LV side. Figure 13 shows that the CCB rides through

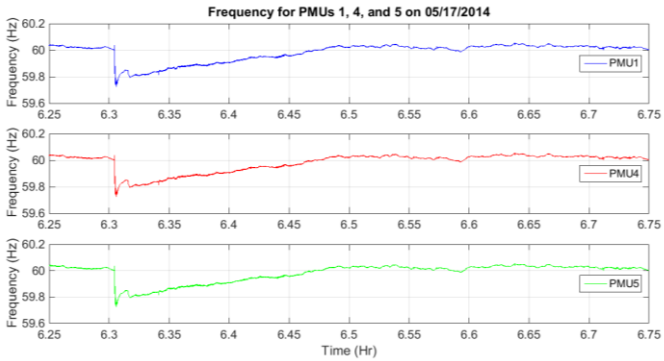

Figure 12. System frequency as measured at PMUs 1, 4 and 5 during a system-level frequency event (another loss of a major win farm).

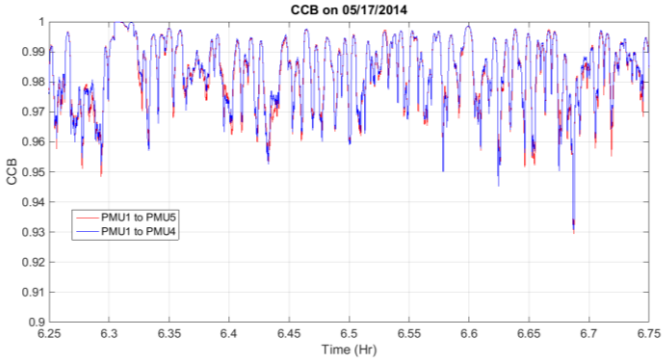

Figure 13. Correlation between the frequencies measured at PMUs 1 and 4 (blue) and 1 and 5 (red) during the event shown in Figure 12.

the event, as desired (in fact, the correlation actually slightly increases during the initial fast downward frequency transient).

It is also important to examine the false trip immunity of synchrophasor-based islanding detection during local events. Figure 14 shows one day from the data set in which there was a very short-duration "spike" in the frequency, at the location indicated by the black arrows. This event was caused by a tripping of one of the inverters in the PV plant while operating at full power. This event does not actually produce a frequency change, but it does produce a momentary jump in phase, and because of the way in which frequency is measured the PMUs interpret this momentary phase jump as a frequency "blip". Figure 15 shows the correlation between the frequencies at PMUs 1 and 4 (blue trace) and PMUs 1 and 5 (red trace). Recall that PMU 4 is on the MV side of the PV

plant GSU transformer, and PMU 5 is on the LV side of that same transformer. For both pairs of PMUs, the result is that the CCB rode

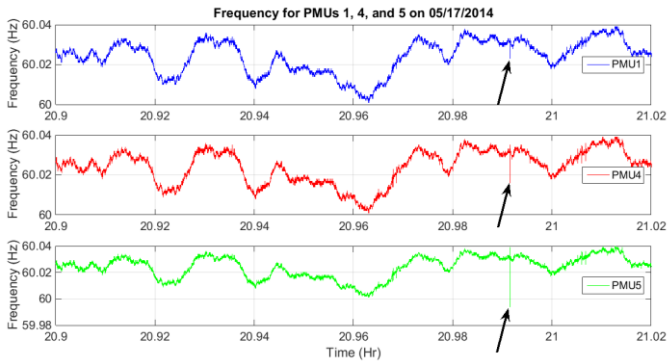

Figure 14. Frequencies measured at PMUs 1, 4 and 5 (top to bottom) for a specific day in the field data set. The black arrows indicate the location of a hairline "spike" in the frequency measurements caused by an inverter trip.

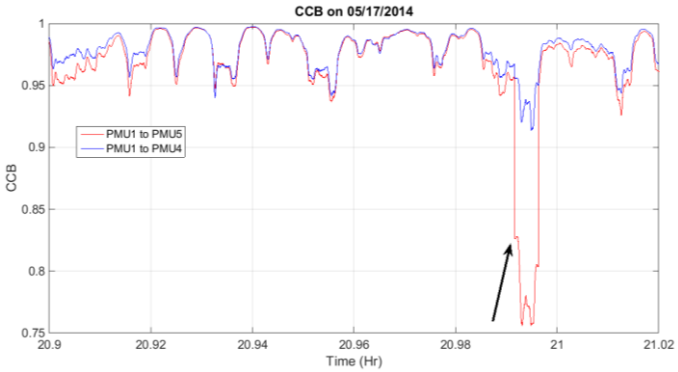

Figure 15. Correlation between the PMU 1 and 4 frequencies (blue) and the PMU 1 and 5 frequencies (red) during the time period shown in Figure 14.

through the event (the CCB trip threshold was set to 0.7), but the frequencies stayed much better correlated when the local PMU was on the MV side of the GSU transformer. Because the triggering event for the spike was on the LV side of the GSU transformer (tripping of one of the inverters), the impedance of the GSU transformer caused the phase jump to be larger at PMU 5 than at PMU 4. This suggests that some design margin could be obtained by placing the local PMU on the MV side of the GSU transformer.

Formal laboratory testing of island detection effectiveness

The CCB + IFE synchrophasor-based islanding detection method was subjected to a set of rigorous and punishing tests at the Distributed Energy Technologies Laboratory (DETL) at Sandia National Laboratories. The testing included four phases.

- Phase 1: standard IEEE 1547/UL 1741 single-inverter anti-islanding testing. (The team also suggested a "Phase 1b" which would be single-inverter anti-islanding testing with a large motor load in the island, similar to the Japanese standard test.)
- Phase 2: multiple inverter testing.
- Phase 3: testing with both inverter-based and rotating machine-based generation.
- Phase 4: false trip immunity testing.

Table 3 shows a sample of results obtained during Phase 1. "ROT" stands for Run-On Time. These results illustrate the conclusion that has been reached over the course of much simulation testing and a limited amount of field tests: in the majority of cases, islands are detected in less than 1 sec, but in some cases, islands do persist for over 4 sec, and in no case does the CCB completely fail to detect an island.

Table 3. Results of Phase 1 testing of the CCB + IFE.

Single inverter tests	
Test #	ROT
1	4.28
5	0.643
6	4.313
7	0.915
8	0.572
Average	2.145
Min	0.572
Max	4.313
SD	1.969

(Note that over the broader set of simulation results, over 80% of the time detection occurs in less than 1 sec. The results in Table 3 were chosen to include some of the worst-case scenarios, but it should not be concluded that the CCB + IFE allows longer than 2 sec run-ons in one-third of test cases.)

Considerable effort has been expended to improve the CCB + IFE's performance in those cases where detection is slower than desired. A screen shot of the frequency vs. time for one of the two cases of a 4+ sec run-on is shown in Figure 16. The blue trace is the local (island) frequency, and the green trace is the remote (grid) frequency. Note that during this test the grid frequency was highly dynamic.

Figure 16. Screen shot of the local (blue) and remote (green) frequencies vs. time during one of the 4+ sec run-ons observed during Phase 1 testing.

In this case, if one considers a windowed average that eliminates the short-term variability of the local frequency, one can see that both the local and remote frequencies

first decrease when the island forms, then increase again, prior to diverging and detection. Visually, there is clearly a significant difference between the local and remote frequencies in that the local frequency has much larger short-term variability than the remote, especially right at the moment of island formation when there is a significant but short-lived dip in local frequency, but the CCB + IFE has difficulty seeing the shorter-term variability because the slightly longer-term trends stay well correlated for a few seconds. It was the CCB that eventually detected this island; Figure 16 shows that the sign of the frequency difference between local and remote frequencies flipped back and forth during the test, so the IFE integrator was partially reset on every change in sign and the IFE response was slowed. The SEGIS-AC team has identified some candidate methods for solving this problem, and these will be evaluated in future work.

The Sandia investigators have also completed a set of ten “Phase 1b” tests with a 10 hp induction machine in the island. Five of these tests involved an unloaded motor essentially acting as a flywheel, and in the other five tests the motor was mechanically loaded. Quantitative results were not supplied, but a qualitative report indicated that in all motor-load cases the CCB + IFE successfully detected the island in well under 2 sec.

The Phase 2 testing has, unfortunately, been relegated to future work due to the high level of difficulty in performing multi-inverter anti-islanding tests.

Representative Phase 3 test results, including a diesel-driven synchronous generator in the island with the inverters, are listed in Table 4. In all Phase 3 tests, the CCB + IFE successfully detected the island. Simulation results and theoretical considerations suggested that detection times might be faster on average with a rotating machine present in the island, and the experimental data collected to date support that conclusion.

Table 4. Representative results from Phase 3 CCB + IFE testing

Inverter + gen tests	
Test #	ROT
2	0.294
3	0.553
4	0.282
Average	0.376
Min	0.282
Max	0.553
SD	0.153

CCB cost analysis

Table 5 shows a bill of materials (BOM) for an implementation of the CCB using 900 MHz radios. The total cost is relatively modest, just under $18,000, assuming that no radio repeaters are required (the need for repeaters would depend on the properties of the microwave path between the substation and the DG site). This cost would be independent of the PV system size, and thus the CCB will be more economical on a dollars-per-watt basis for larger systems. To illustrate this, Table 6 shows the CCB costs for three different PV system sizes. As noted in the final column of Table 6, for a 500 kW plant, this analysis suggests that deploying the CCB would cause the PV price in $/W to go up by about 16% relative to the cost without the CCB, which is not acceptable and indicates that a less expensive solution is still desired. For a 2.5 MW PV plant, the cost escalator is only 3.5%, which is much more tolerable but still could be improved, and the escalator is only about 1% for the 10 MW plant.

Table 5. Bill of Materials for an implementation of the CCB using 900 MHz radios.

Hardware	Qty	Price per unit	Total Price
SEL-3031 Serial Radio w/ Enc Card	2	$1,223.00	$2,446.00
SEL-351A Relay (not Legacy SEL-351A unit)	1	$1,260.00	$1,260.00
SEL-700 GT Relay	1	$2,500.00	$2,500.00
SEL-2401 GPS Clock	2	$498.00	$996.00
SEL-3530 RTAC	1	$2,850.00	$2,850.00
15kV Class PT	6	$1,100.00	$6,600.00
Heavy duty COTS Backup Power Supply	2	$250.00	$500.00
Antenna Cabling, Hardware, etc.	2	$200.00	$400.00
	Total		**$17,552.00**

Table 6. Incremental cost of adding CCB cost to three different-sized PV plants, on a $/W basis.

Number of inverters	Total plant size (kW)	Cost/W per inverter	Total plant cost	CCB cost/W	Total plant cost/W	Cost with CCB relative to cost without
1	500	$0.22	$110,000.00	$0.04	$0.26	115.96%
5	2500	$0.20	$500,000.00	$0.01	$0.21	103.51%
20	10000	$0.17	$1,700,000.00	$0.00	$0.17	101.03%

However, note that this analysis assumes that all of the CCB components are being installed specifically for the purpose of implementing the CCB. One of the key advantages of the CCB, relative to DTT or Power Line Carrier Permissive (PLCP), is that at least in theory the CCB could take advantage of relaying equipment already present on the feeder. Table 7 shows the CCB BOM again, except in this case it is assumed that the feeder head-end relay already exists, which in most cases it would. (Any substation engineering cost is excluded here, and by way of full disclosure it should be noted that this substation engineering cost can be substantial. That factor is excluded here because it is highly site-specific and utility-specific.) Table 7 also assumes that the relay at the DG plant also already exists, which is based on the assumption that the utility will require a redundant relay for the PV plant. This is a likely scenario for most utilities and for most PV plants of size 500 kW or larger. Table 8 shows the incremental cost of adding the CCB as a function of PV size, with the assumptions from Table 7. Table 8 shows a much more favorable cost comparison; even at the 500 kW size level the CCB cost escalator is only 6.5%, which is much more tolerable, and it is only about 1.4% for the 2.5 MW plant and 0.4% for the 10 MW plant.

Table 7. Bill of Materials for a CCB installation, assuming that the feeder head-end relay and the DG site redundant relay already exist.

Hardware	Qty	Price per unit	Total Price
SEL-3031 Serial Radio w/ Enc Card	2	$1,223.00	$2,446.00
SEL-351A Relay (not Legacy SEL-351A unit)	1	$1,260.00	$1,260.00
SEL-700 GT Relay	1	$2,500.00	$2,500.00
SEL-2401 GPS Clock	2	$498.00	$996.00
SEL-3530 RTAC	1	$2,850.00	$2,850.00
15kV Class PT	6	$1,100.00	$6,600.00
Heavy duty COTS Backup Power Supply	2	$250.00	$500.00
Antenna Cabling, Hardware, etc.	2	$200.00	$400.00
	Total		**$7,192.00**

Table 8. Incremental cost of adding the CCB to PV plants of various sizes, on a $/W basis, using the cost value from Table 7.

Number of inverters	Total plant size (kW)	Cost/W per inverter	Total plant cost	CCB cost/W	Total plant cost/W	Cost with CCB relative to cost without
1	500	$0.22	$110,000.00	$0.014	$0.23	106.54%
5	2500	$0.20	$500,000.00	$0.003	$0.20	101.44%
20	10000	$0.17	$1,700,000.00	$0.001	$0.17	100.42%

Task 2: Advanced Inverter Functional Controls on Fielded Systems

Smart inverter functionality was becoming a big topic in the solar industry around the start of the SEGIS-AC program. Some smart inverter functionality had been demonstrated by the time the program FOA came out, and various working groups were grappling with the issues associated with high penetration of PV, looking at worldwide progress in this area and defining the meaning of “smart inverter”. In short, “smart inverter” in this context means a PV inverter that has commanded or autonomous control capability to facilitate enabling higher penetration of PV on feeders by mitigating the issues associated with PV such as intermittency, over generation, voltage rise and other related grid issues. For this task the focus was to take earlier smart inverter developments, further define and refine capability sets based on industry progress, qualify functionality in 3rd party labs, and ultimately to field demonstrate it. Additional topics to be covered included looking at impacts on utility feeders such as distribution switchgear cycles and overall voltage regulation.

Standards and industry development

During the program many developments unfolded related to enabling increasing amounts of PV on the grid by utilizing smart inverter functionality. The team studied the

German interconnect standards including the medium voltage directive. Active participation on the EPRI smart inverter working group and the IEEE1547a committee proved invaluable in understanding utility concerns as well as providing input to the group in a number of areas. Some of the key focus areas included helping utility experts who didn't know a lot about PV inverter technology understand capabilities and limitations of PV inverters. The team also worked to ensure that the emerging standards were not too prescriptive in addressing grid management concerns. As penetration levels continue to increase, the team wanted to allow other forms of island detection for instance, so the team worked to ensure communications based techniques would not be dis-allowed in the written standards. It also became clear from customer and utility interactions across North America that a one size fits all Smart Inverter would not be possible. A flexible suite of solutions would be needed. This informed development, understanding that a platform based approach would be needed enabling functionality that could be autonomous or commanded. In addition to EPRI and IEEE1547a, many other groups have been grappling with the issues of high penetration and throughout the program the team kept abreast of the latest thinking, approaches, and requirements. These groups include the CPUC Rule 21 committee, island interconnect requirements (specifically HECO), the Northeast Power Coordinating Council (NPCC) and others.

Solution development

One way to look at the needs for smart inverters is to categorize the functionality. Below is a category map of the functionality:

Need	**Function**	**Autonomous**	**Commanded externally**
Do not trip offline when generation is needed	Low and high voltage ride through	Must be inverter integrated, hardware and software implications	Too slow
	Low and high frequency ride through		

Need	Function	Autonomous	Commanded externally
Mitigate intermittency induced voltage problems	Voltage support	Volt/var, volt/watt	SCADA fixed or closed loop control; slow or relatively high speed (<10Hz)
Disconnect when isolated from utility, micro-grid operation	Island detection	[3]Various inverter integrated algorithms including Sandia Frequency Shift and Impedance Detection	CCB, power line carrier, transfer/trip
Mitigate intermittency induced frequency problems	Generation balancing (droop controls). Only effective for upward frequency excursions unless storage is included.	Freq/watt	SCADA fixed or closed loop control

Table 9: Smart inverter functional needs and solution approaches

Table 9 above illustrates the host of utility needs related to intermittent distributed generation sources and the possible solutions or mitigations to these needs. Depending on penetration level, plant size, infrastructure capability and a host of other factors, the utility (and the PV plant developer) must make a combination business/technical decision on how to address the need. Thus a configurable platform approach makes sense enabling broad flexibility and choice maximizing the possible implementations allowing customers to identify the most effective solution for their specific need.

An inverter platform had been developed in the earlier SEGIS program that enabled flexibility and rapid development while minimizing the need for repeated re-certification often needed with inverter platform software changes. A two processor solution was employed with one processor focused on mission critical inverter controls and supervision and the secondary processor focused on the SCADA interface and the configuration interface for autonomous and fixed mode controls. This secondary

[3] Ropp, W. B. (n.d.). *Evaluation of Islanding Detection.* Retrieved from http://prod.sandia.gov/techlib/access-control.cgi/2002/023591.pdf

controller would not be subject to the same level of scrutiny from certification bodies enabling flexibility to make rapid changes.

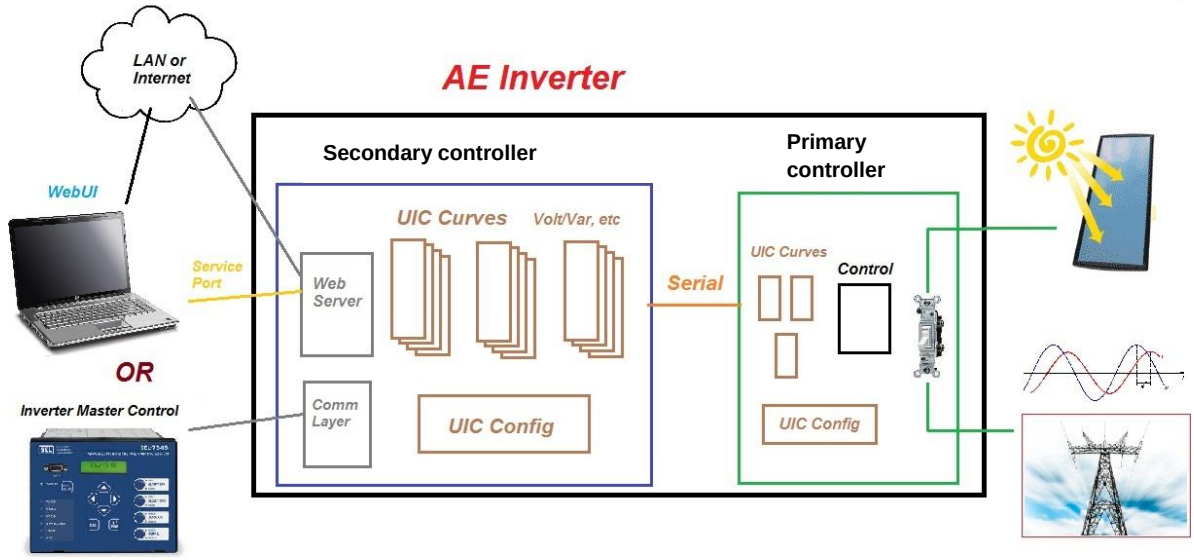

Figure 17: Configurable smart inverter platform

The diagram above illustrates the configurable platform in which the primary controller performs primary control functions (highest speed critical functions) and is subject to UL1741 certification. The secondary controller does not require waveform synthesis (inverter functionality) or safety and utility interconnect related functions enabling it to be modifiable without requiring standards body review upon iteration. This flexibility allows a relatively small code footprint to be hardened and proven and changed infrequently while allowing the secondary controller code to be more fluid allowing adaptation to the evolving grid integration needs.

Inverter autonomous controls

Inverter autonomous controls represent a significant area of development for the various smart inverter working groups (EPRI, IEEE1547a, CPUC, and others). Autonomous controls enable inverters to provide some level of grid support and intermittency mitigation without the need for supervisory control of any kind. While autonomous controls are still minimally used in North America at the time of writing this report, this type of control represents the next step in enabling higher penetration of PV because smaller systems that cannot economically support external control can still provide the controls needed to enable installation on feeders that utilities deem unable to accept any more PV without some form of utility interactive controls. In many cases we see fixed power factor, VAr or curtailment at sites of this nature. Inverter autonomous controls represent the next logical step.

One exception is ride-through. Voltage and frequency ride through have been used within the industry for some time. This autonomous control amounts primarily to a widening of trip points enabling the inverter to “ride through” most grid transients instead of disconnecting and potentially contributing further to a voltage surge or collapse. Ride through typically voids the UL listing based on the current interconnect standard IEEE1547, and this has limited widespread deployment of this functionality. AE inverters can be purchased with ride through functionality and this functionality has been demonstrated both in the field and in laboratory environments. The core logic associated with measuring grid voltage or frequency and comparing it with the ride through envelope and ultimately disconnecting or riding through is all built into the primary controller. However, the configurability (e.g. the ride through envelope setpoints) are all housed in the secondary controller enabling configurability without requiring a costly relisting process. Figure 18 below illustrates a typical ride through curve as seen through the integrated web UI of the secondary controller.

Figure 18: Configurable voltage ride through envelope

The remaining autonomous functions with the exception of island detection covered at length earlier in this report are Volt/VAr, Volt/Watt, and Freq/Watt. Most of the work was focused on Volt/Var and Freq/Watt since Volt/Watt is expected to be a less common function, because most feeders have a relatively high X/R ratio implying that Volt/VAr would be much more effective at line voltage regulation than Volt/Watt.

Figure 19 below illustrates a sample configurable Volt/VAr profile. Curves for Volt/Watt and Freq/Watt are configurable in a similar way via the same web enabled user interface shown here. For each of these autonomous control functions, the secondary controller provides the visualization and configurability while the primary controller maintains the current operating set and performs the actual control functions (e.g. at grid voltage x, export y VAr's.

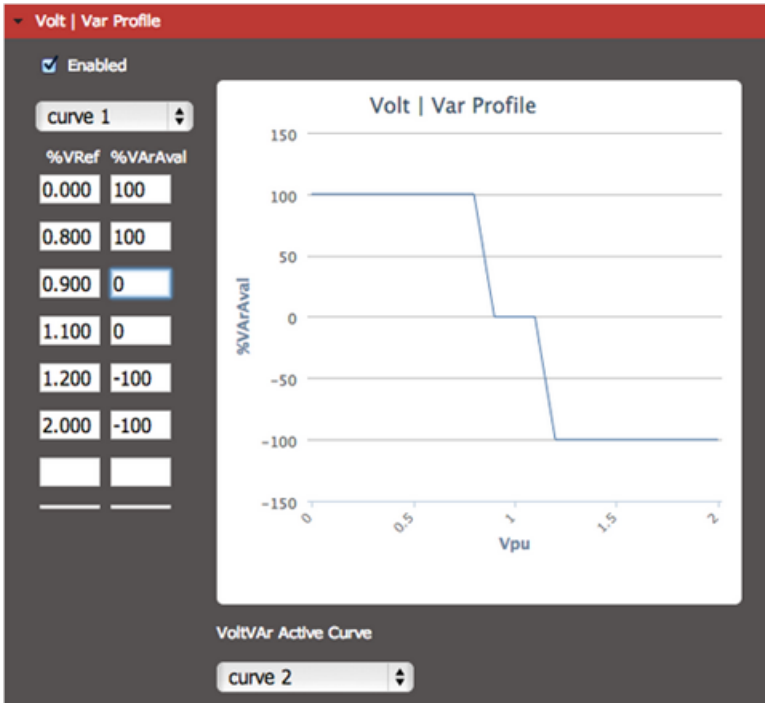

Figure 19: Example of a configurable Volt/VAr profile on an AE1000NX inverter

The autonomous control functionality was demonstrated at Advanced Energy's laboratories, but also thoroughly evaluated at NREL's ESIF (Energy Systems Integration Facility). Tests were performed with a DC power source and an AC grid simulator with the inverter running at various power levels. The grid simulator would be programmed for a voltage sag or swell or a frequency sag or swell and the inverter response would be recorded. Figure 20 below illustrates a 50kW inverter's Volt/VAr response to a grid voltage sag. Note the voltage sag and subsequent VAr output response. The yellow is the grid voltage and the green is the AC output current from the inverter. Note that the current is nominally constant through the sag event, but the current begins to lag the voltage waveform as the grid voltage sags illustrating the expected behavior based on the programmed Volt/Var curve.

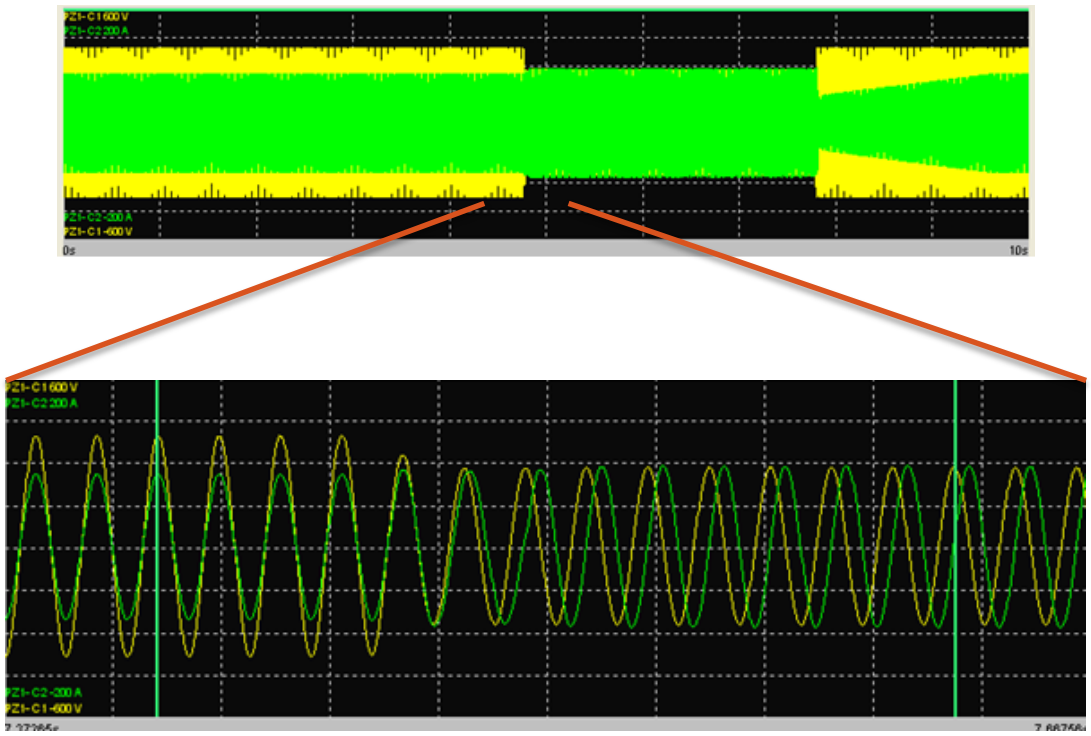

Figure 20: Inverter Volt/VAr response to a grid sag event

Each of these autonomous functions can be configured and enabled or disabled independently via the integrated interface. The Freq/Watt and Volt/Watt curves and inverter response results are similar. For brevity, results from these autonomous control functions have been omitted. Note for VAr/PF control, additional flexibility was built into the platform to enable prioritization of real or reactive power depending on the needs of the PV plant.

Most smart inverter working group standards development allows for autonomous control functionality, but standard profiles have not yet been developed, and in fact as described earlier in this report, a one size fits all set of profiles simply isn't practical due to the uniqueness of various utility distribution systems. This was one of the driving reasons for developing and providing a flexible platform based approach. At the time of writing, most PV systems are being installed with simple SCADA controls, or fixed power factor. Few if any installations are leveraging autonomous volt/var or freq/watt beyond a few utility scale plants that use LVRT coupled with a VAR support on LVRT event. Development of these controls has been done consistent with industry standards as well as emerging communications interface standards for management of these functions (SunSpec and IEC61850).

Externally commanded controls

In addition to autonomous inverter controls, supervised control (from an external controller) is also often needed and where economically feasible can provide a better level of control stability. Most large PV plants have SCADA control and often some kind of power factor correction or voltage control scheme to minimize the impacts of intermittency and also to offset the magnetizing inductance associated with the transformer coupling of the PV system to the medium or higher voltage utility transmission and distribution system. The secondary controller platform in the inverter was designed to accommodate this form of externally commanded control.

The team focused on driving PCC level control capability to the system enabling Volt/VAr, Frequency/Watt, and Volt/Watt from the Schweitzer RTAC (master controller). All three functions were implemented and tested within the AE laboratory with loop rates of 10Hz. Implementing these functions at the PCC enables a coordinated approach consistent with the needs of medium to large scale solar deployments where inverter based autonomous smart inverter controls could be difficult to realize due to issues of approximating PCC voltage at the inverter terminals and risks of inverter to inverter interaction. This control scheme represents a logical step towards leveraging higher speed inverter control (rather than traditionally low speed SCADA coordinated control), but addresses the issues mentioned associated with a large number of inverters at a single site running autonomously without central coordination. This approach also enables the controller to work with various DER assets that have a communications interface, enabling the master controller to drive Volt/VAr, Frequency/Watt, and Volt/Watt on all assets capable of commanded VAR and power level.

In Figure 21 below is a chart of the Volt/VAr control illustrating a simulated voltage ramp in green, the corresponding kVAr response in blue, and the actual system voltage change in red. Actual voltage change is very small, only a volt or two in AE's lab due to the low impedance grid source. This control was implemented as PCC level control, looking at a local meter (PMU) to get system voltage and adjusting the VAr output of any number of inverters based on the Volt/VAr curve. Typically the VAr output would be divided evenly amongst all connected resources, but it could also be divided up due to various site needs or constraints. It should also be noted that the "PCC" could also be a remote control point anywhere within the utility distribution system enabling wide area control capability.

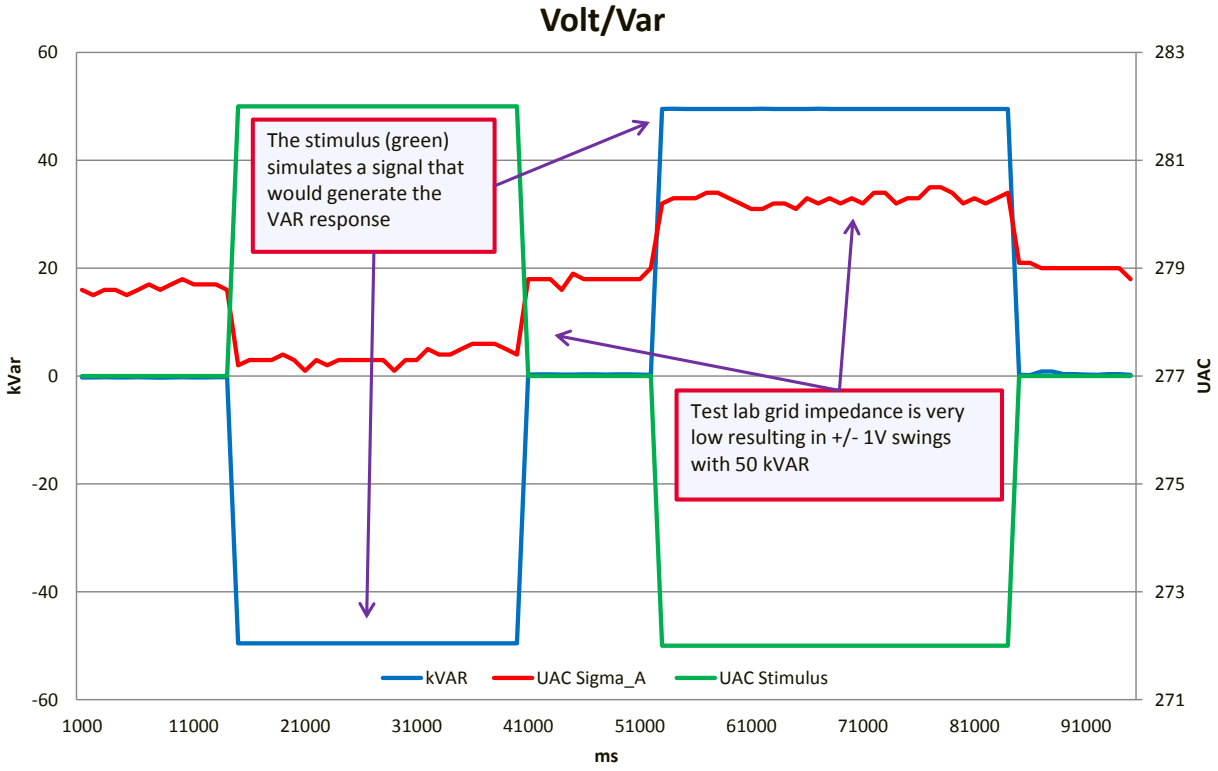

Figure 21: Demonstration of PCC level volt/var in AE test lab

Field and laboratory testing results

With a flexible controls platform in place, laboratory and field testing encompasses the primary remaining step. During the program, smart inverter voltage support functionality was implemented on all AE product lines and tested not only in the AE facility, but at Sandia and NREL labs.

Additionally, in terms of field demonstration/validation, the Canby-Butteville feeder was studied to determine the impacts of voltage support functionality (see Task 0 above), and VAr control tests were performed on the feeder to verify the impacts on system voltage met expectation based on the model. This was done with the existing PV inverters onsite and modeled to determine expected impact of VAr control with the additional BIS that was planned to be installed at the Baldock site. The Canby-Butteville feeder was instrumented with 5 PMUs distributed along the feeder from the substation to the PV plant (see details in Task 0 above). Data was routed via wireless and concentrated at the Baldock site and then transferred via fiber link to PGE's headquarters. In Figure 22 below, a 1.5 hour time window is captured illustrating the voltage response to the following stimulus provided by the PV inverters at the Baldock plant. The inverters were commanded to ramp reactive power slowly beginning at 18.7 GMT continuing through to 18.9 GMT consuming reactive power. The plant was then

commanded back to full real power. Following the ramp, there exist 5 step changes in reactive power:

1) 500 kVAR consuming
2) 0 kVAr
3) 1 MVAR consuming
4) 500 kVAR consuming
5) 0 kVAr

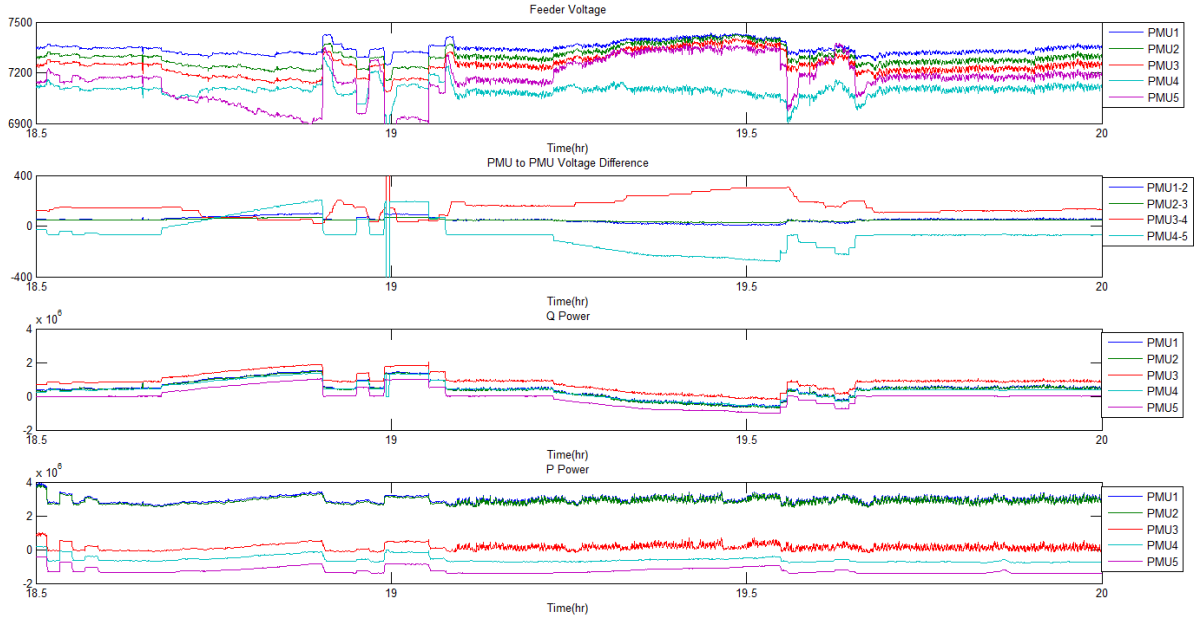

Figure 22: Canby-Butteville PMU measurements over 1.5 hr test window

During the step changes there exists significant deflection in the PMU system line to neutral voltages across the entire distribution circuit. The system voltages (depending on which PMU you are monitoring) are all pulled down, even the one at the substation. The testing continues as a ramp in reactive power is commanded starting at approximately 19.2 GMT and continuing through 19.6 GMT to allow the regulators appropriate time to react to the reactive power loading and maintain the proper system voltages. At 19.6 GMT a series of steps in sourcing reactive power are accomplished, again step sizes chosen as to not exceed regulator timing and cause an out of range voltage event for the connected customers. One noteworthy effect of commanding absolute reactive power is the reduction in real power as the inverters are kVA limited at their nameplate rating (260 kVA). This does offset the total impact to the circuit, however with reactive power being the primary driver of system voltage it can be considered a second order effect. Figure 23 highlights the system voltage deflection at PMU 4 vs. reactive power output from the site.

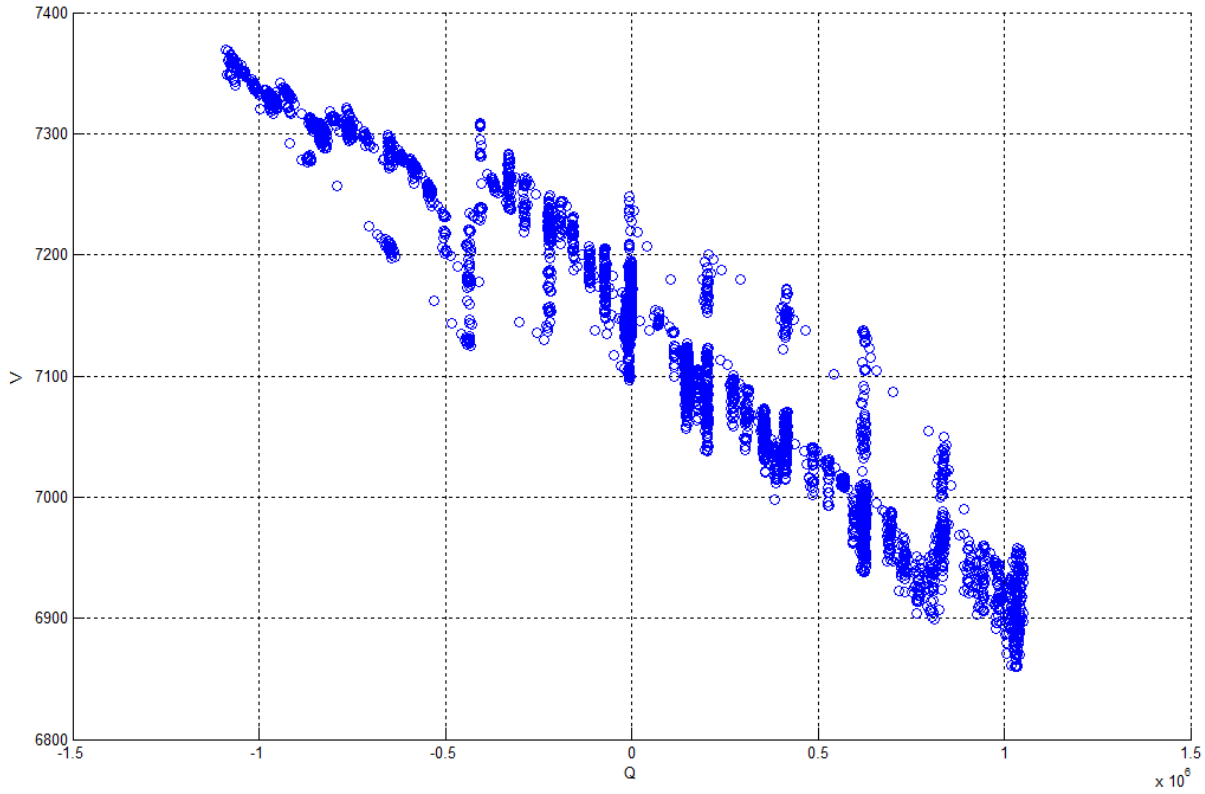

Figure 23: Feeder voltage response to Baldock reactive power stimulus

What is evident from this plot is that the reactive power output at the site has significant impact on the system voltage up to the set of single phase voltage regulators. Mapping the absolute phase-to-neutral voltage at PMU 4 to the reactive power leads to a (7350-6850) 500 volt deflection over a +- 1MVAr relative change in reactive power. This is a (500/7200) ~7% voltage change when allowing for the regulators to ratchet, and more significant if accomplished without waiting for the system to stabilize. This voltage response is also consistent with the results of the Volt/VAr modeling work discussed in Task 0 suggesting that a specific Volt/VAr scheme deployed at Baldock could make a positive impact on overall feeder performance, while reducing voltage regulation equipment cycles.

One last item to note in Task 2 is the development and accomplishments made with the NREL team in Power Hardware In the Loop (PHIL) testing. PHIL testing represents a powerful way to test real hardware (inverter) in the loop and leverage existing feeder models enabling full testing of the inverter's response to various feeder configurations and operational scenarios. Both the Baldock and Minnatola South feeder Matlab models were used in the PHIL lab at NREL, coupled with an AE500TX inverter. At the time of writing this report, preliminary results were available showing good correlation between traditional laboratory testing and PHIL. This work was not completed during the

SEGIS-AC program, but represents significant advancement in methodology to test complex systems and utility interactive control schemes in the lab under various scenarios before they are run on a live feeder where unexpected operation can be extremely costly.

Task 3: Ramp Rate Controller

In this task the team set out to develop a symmetrical ramp controller to mitigate the effects of cloud induced transients. Upward ramp rate limiting functionality had been available in PV system controls for some time, but without storage, downward ramps could not be mitigated. The team wanted to understand the benefits, costs, and constraints associated with development and deployment of a symmetrical ramp controller, which to realize requires a bi-directional inverter and storage system. This task required significant development compared to Tasks two and three, which were closer to demonstration readiness. Thus the team defined this body of work starting with the fundamentals of understanding power ramps at the candidate demonstration site (Baldock – on the Canby Butteville feeder), as well as gaining a better understanding of real utility concerns and requirements around power ramping on their grid. This information would then be synthesized into requirements for the battery, storage inverter, and ramp controller. Finally, once developed the team would lab and field demonstrate the storage system and present major results and opportunities to move the technology into industry. The following sections describe the phases of work, major milestones, results, and setbacks that the team covered throughout the SEGIS-AC program.

Understanding ramps

To start, the team set out to understand ramp characteristics and requirements in two areas:

1. Range of power ramps experienced at the Baldock demonstration site
2. Utility mindset and requirements towards power ramps on their feeders

The first task was relatively straightforward. The team leveraged the installed PMUs at the Baldock site and captured power versus time data for several months. Once a representative dataset was available, the team analyzed the data to understand the ramp content by binning the data across the spectrum of possible upward and downward ramps. The figure below illustrates seven months of power ramp data binned into a histogram in 100kW/min ramp bins. From the chart it is immediately obvious that more than 99% of the ramps are within +/- 300kW/min (5 kW/sec). What is not directly evident in this chart is the additional fact that more than 97% of the ramps were relatively shallow in depth, with an irradiance change of less than 30%, enabling a

300kW battery power rating to accommodate the vast majority of the downward ramps. The low power level needed to accommodate the ramp controls at Baldock was counter-intuitive as one would typically assume a need for a battery corresponding to an 80% irradiance change (approaching the 1.4MW plant power level); especially with how slow the recorded ramps were. The reality however was that most ramps were not very deep, so for the weather patterns experienced at this site, a 300kW rating met the requirement to cover the vast majority of the ramps.

One other notable item: First principles analysis was also used to estimate worst case ramp rates and depth based on the PV panel rating, geometrical layout, cloud velocity and approach. This analysis suggested a maximum theoretical ramp rate of 193 kW/sec, and an irradiance depth corresponding to nearly the full rating (1.4MW) of the power system. This conservative approach would lead to a significantly more expensive battery for ramp controls that would ultimately be oversized for the real world ramping and cloud depth conditions at the site. Conclusion: Getting real site data is critical to optimal cost-effective BIS sizing.

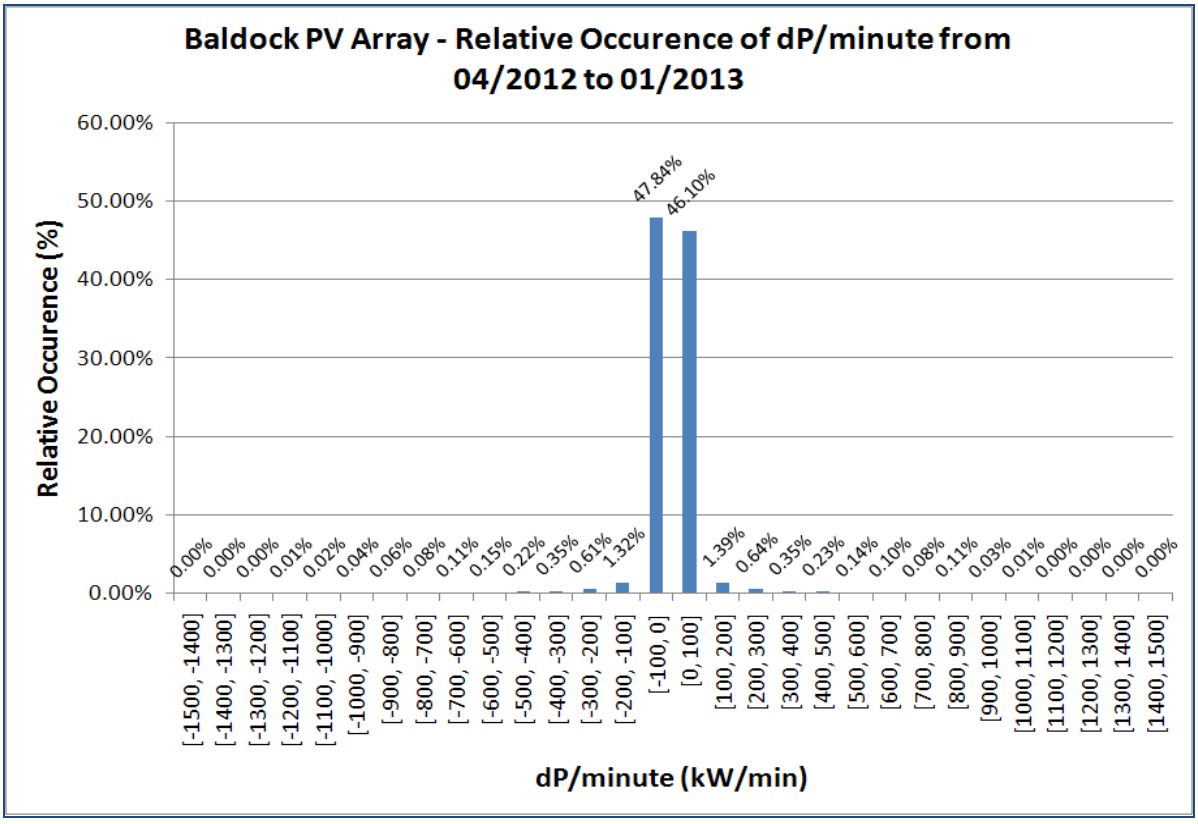

Figure 24: Histogram of ramps at Baldock PV plant over 9 month period

Once the power rating had been determined, the team set out to determine the energy rating for the battery. The team looked at theoretical and empirical approaches to sizing

the battery. Ultimately an empirical approach led to a result best suited for the Baldock site. Below is a figure that illustrates the energy needs throughout most of the year on a month by month basis assuming the 300kW battery power level and a target ramp rate of 1kW/sec. Each month's data was processed on a day by day basis and then monthly, tracking the absolute worst case energy needs to maintain symmetrical ramp control at 1kW/sec. The data illustrates that a 300kWh rating would meet energy needs even on the worst day of the worst month in June where there was an energy excursion of 276.4 kWh (165.8+110.6 kWh).

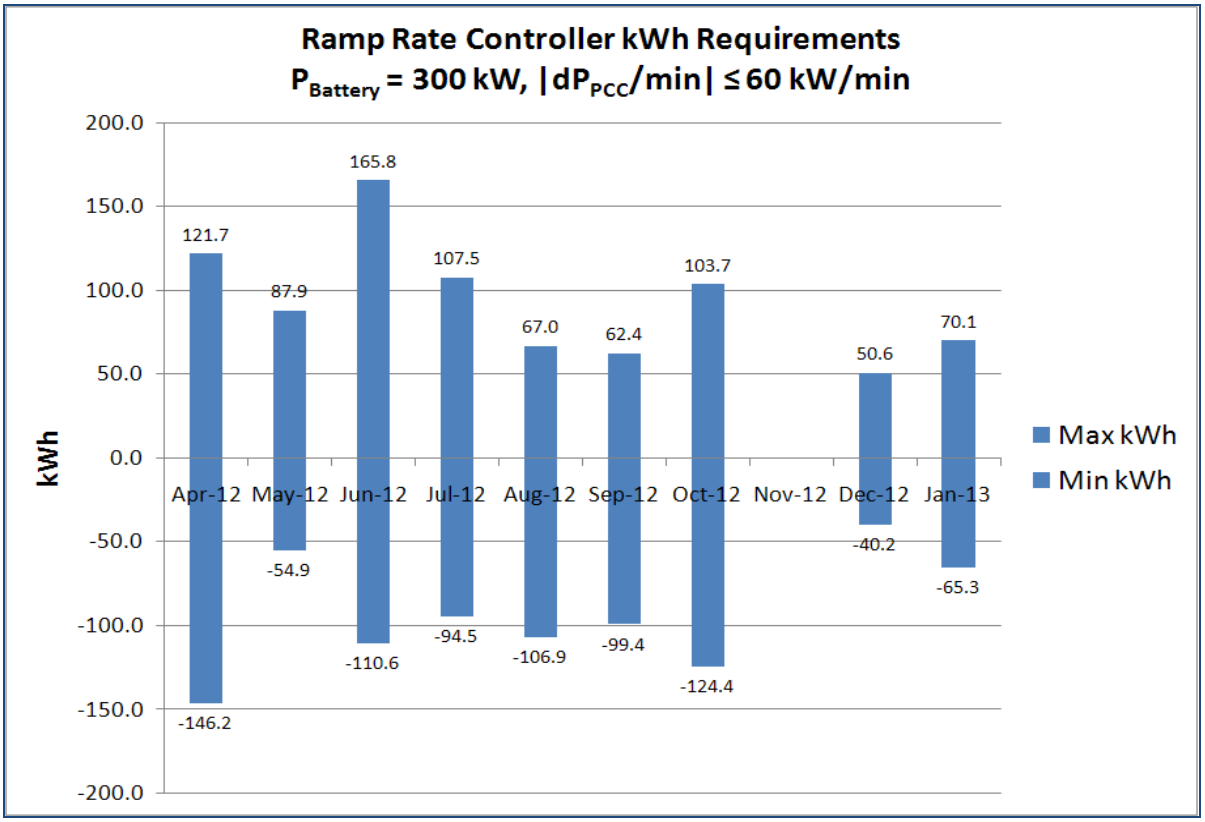

Figure 25: BIS energy requirements for 60kW/min ramp setting, Baldock PV plant, 9 of 12 months

The second task the team set out to accomplish in understanding ramp characteristics and requirements was to better understand various utility considerations around power ramps on their network. Through a combination of research and discussions with grid operators (specifically at PGE), the team attempted to identify a hard requirement for the ramp rate limit. It turns out that this is not such a straightforward question to answer. Grid operators fundamentally are concerned with voltage regulation or area control error (ACE) and frequency regulation. Both must be kept within set limits or the operator can be penalized financially and even worse, there is a possibility for customer equipment damage if frequency or voltage become severely out of range. To translate

this into a ramp requirement for the PV plant, one must characterize the potential impact of the plant on ACE and system frequency. This is a function of many factors, but generally comes down to balancing generation with load. Utility assets are somewhat limited in their ability to ramp up their output powers. Table 10 gives representative values for the ramp rate capabilities of typical utility generation assets. A sudden irradiance drop at the Baldock site must be compensated for with an equal and opposite generation increase (or load reduction) somewhere in the control area. Generally load decrease is not under the utility's control, and increase can be provided, but traditional generation ramp capability is relatively slow. The table below illustrates typical generation ramping capabilities. A typical 500MW combined cycle gas-fired would be able to compensate for a single 1.4MW PV plant easily at its 4%/min (20MW/min) ramping capability, but would quickly become far too slow if a large amount of PV were employed (a 200MW plant, or 200MW of PV in the control area) might ramp at roughly 30-50MW/min based on the irradiance change profiles from Baldock, leaving the gas-fired plant unable to effectively compensate.

Table 10: Operational characteristics of conventional generation sources

	Nuclear	**Hard Coal**	**Lignite-fired**	**Combined cycle gas-fired**	**Pumped Storage**
Start-up time "cold"	~ 40 hr	~ 6 hr	~ 10 hr	< 2 hr	~ 0.1 hr
Start-up time "warm"	~ 40 hr	~ 3 hr	~ 6 hr	<1.5 hr	~ 0.1 hr
Load gradient "nominal Output" ↗	~ 5%/ min	~ 2%/min	~ 2 %/min	~ 4%/min	>40%/min
Load gradient "nominal Output" ↘	~ 5 %/min	~2 %/ min	~ 2 %/min	~ 4%/ min	>40%/min
Minimal Shutdown time	← Not applied →				~ 10 hr
Minimal possible load[4]	50 %	40 %	40 %	<50 %	~15%

[4] This value is determined by efficiency and economic constraints and this thus more of a "minimum feasible load" than a "minimum possible load". When loaded below the "minimum possible load" value in the table, the efficiencies of the power plants drop rapidly by as much as 5 to 20% absolute.

By providing predictable symmetrical ramps enabled by storage, the utility can better plan for and utilize higher amounts of intermittent resources as well as utilize conventional generation to compensate for irradiance ramps. Setting the ramp requirement is still complex and a function of many factors specific to the control area. For Baldock, the team arrived at a ramp requirement for demonstration of +/- 30kW/sec. This decision was not completely arbitrary, but was also not based on a hard requirement since the Baldock plant couldn't really affect ACE or system frequency on the Canby-Butteville feeder because of its small size relative to the size of the interconnected system. The 30kW/sec number was a good balance between the capability of the battery, typical generation ramping capabilities, and then-existing world-wide ramp requirements based on a survey the team did during the program. Penetration levels of PV are quite low in the PGE control area so a slow ramping requirement simply wasn't needed, and local grid operators agreed 30kW/sec would be a good target for the demonstration.

Once the critical battery parameters had been identified, a battery vendor was needed. Other than traditional lead acid battery solutions, the battery market has been very much in flux in terms of technology and cost evolution. The team wanted an established vendor and partner to provide the battery and ultimately selected Saft as the partner given their track record and history of supplying battery systems. The 300kW/300kWh battery specification was defined and quoted by Saft. Since the team adapted a 600VDC- 500TX PV inverter for this application, the typical Saft battery system configuration was modified to work with a 600V maximum DC input configuration required by the AE500TX inverter platform.

Ramp controls development

As mentioned above, the team selected an AE500TX platform to modify for storage use. Additionally, an SEL RTAC-3530 real time automation controller was identified for the system ramping controls implementation. The AE500TX controls were modified to enable 4 quadrant operation, and proper hooks were put in place to enable charge and discharge commands as well as general operation with a battery source rather than a PV source. The Saft battery came equipped with a CANbus and CANopen stack. The AE500TX was selected also because of its availability of a CANbus port. The CANopen stack was implemented on the AE500TX enabling it to retrieve and set battery parameters. Unfortunately, the RTAC did not have CANbus capability so the team selected a National Instruments cRIO as a flexible middle layer to provide protocol translation (CAN to Modbus) as well as some glue logic. Over the course of the program it became clear that the cRIO would be a better choice for the system control and ramp algorithm development and the team eliminated the RTAC, simplifying the overall system design.

Once all the functional components were in place and the base capability set was built into the inverter and cRIO, the team was able to focus on the ramp controls. Simulink was employed to model various types of ramp limiters. Achieving consistent and stable ramp control the traditional way using a closed loop ramp limiter looked difficult both to implement and to achieve consistent and reliable stability. The team looked at alternatives and hypothesized that a smoothing controller might ultimately provide similar results and could potentially be implemented far easier and with a much higher likelihood of consistent, reliable operation. The basic concept of a smoothing controller is to look at the PV output and smooth it moment by moment (we chose a single time constant IIR digital filter) with the appropriate time constant (derived from the ramp control setting). Differencing the smoothed PV from the actual PV output effectively becomes the storage output setpoint. This approach proved far more straightforward and in fact provides a response more similar to how traditional generation would react to compensate. While there is some phase delay, it provides no measurable impact or concern on the aggregate output of the system. In the smoothing controller case, the BIS operates essentially as an active filter, rather than an active ramp limiter.

The team ran a 5 second interval data set from a Duke territory PV site through the Simulink model and demonstrated properly smoothed output behavior. The two figures below illustrate the before and after smoothing pictures for the solar day, which was a mix of clouds and sun. Once the smoothing algorithm had been developed and tuned, the team was able to port it to the cRIO platform.

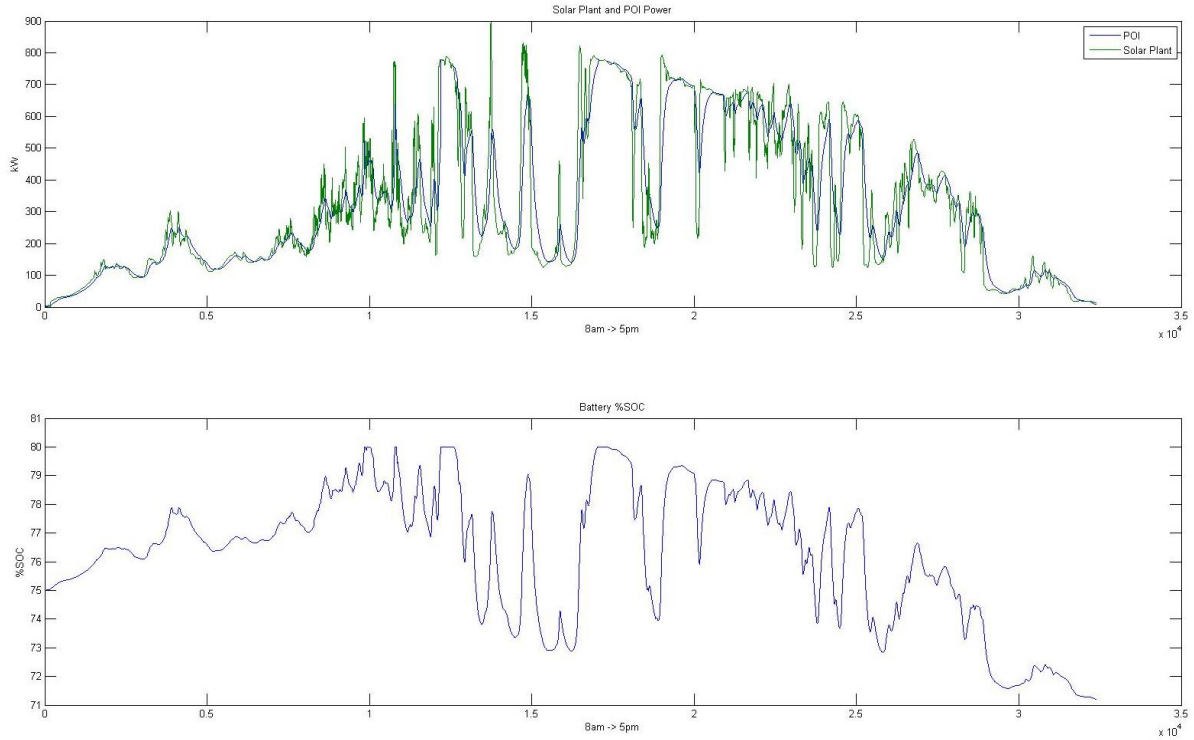

Figure 26: Top plot - actual Duke PV system 5 second output 12/31/14 and smoothed output. Bottom plot - SOC profile for given ramp coefficient

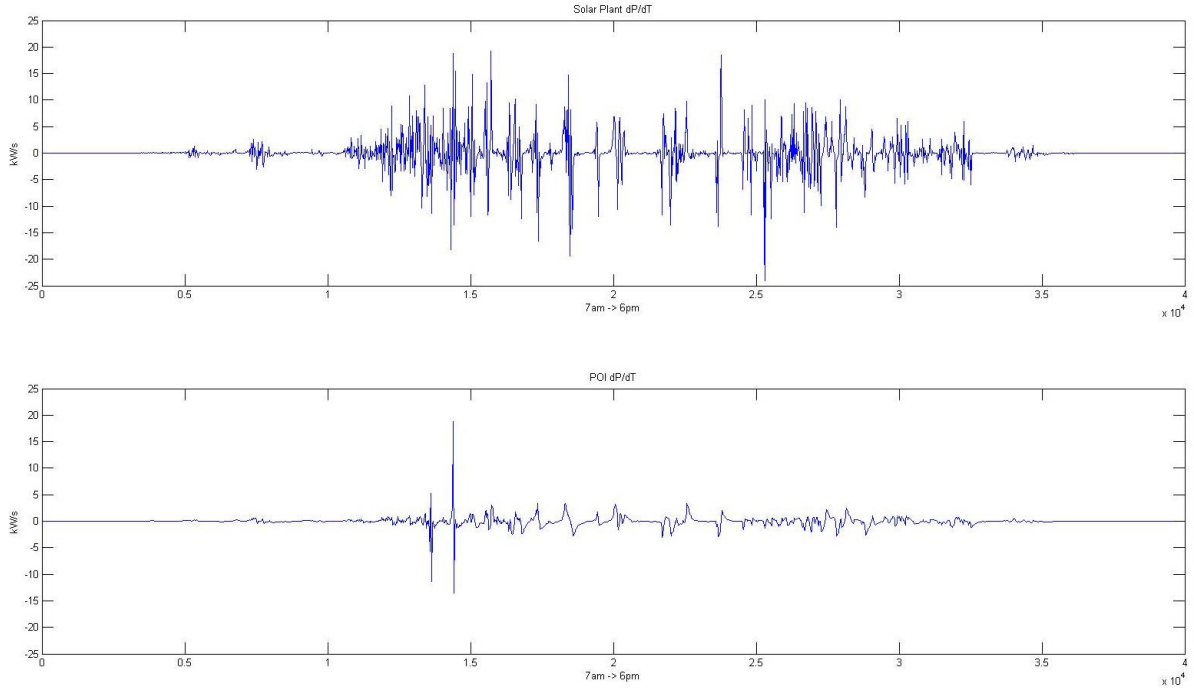

Figure 27: Top plot - PV ramps throughout the day. Bottom plot - POI ramps after smoothing applied by BIS

Ramp controller operation

The diagram below illustrates the components in the system including the PV system and inverter, the point of interconnection, the connected PMU's, the BIS, and the cRIO system controller. The cRIO communicates with each meter (PMU) as well as the BIS over CANbus. This particular site has two PV systems, one with a central inverter, and one with string inverters, so a PMU at each PV output is employed, and the cRIO sums the two outputs together to get the aggregate PV output. The cRIO monitors the PV output, filters it, and defines the output at the POI by setting the storage inverter output.

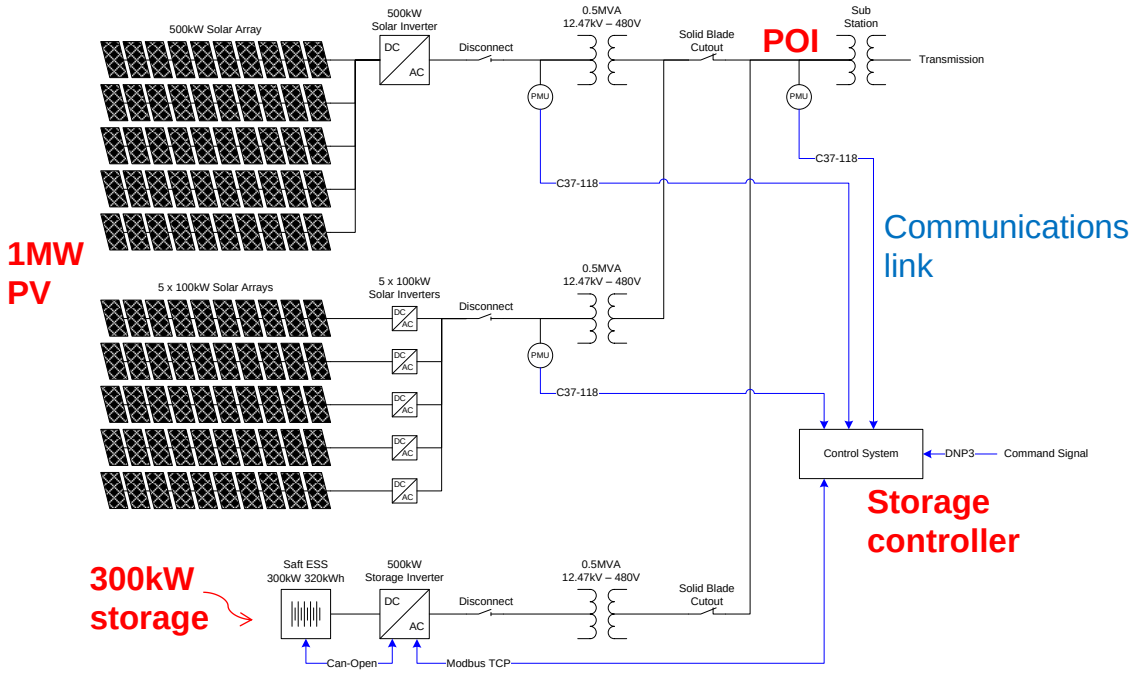

Figure 28: Block diagram for a typical system with ramp controls illustrating POI, PV system, and BIS

Once the controls capability was implemented in the cRIO, the team used the 5 second solar dataset shown earlier and simulated the PV output by feeding the dataset into the cRIO. The cRIO then performed the smoothing, set the BIS output appropriately (actual 50kW Saft battery and 50kW inverter) to achieve the smoothed response at the POI. The screen shot below illustrates actual output of the BIS and calculated POI output based on the input PV dataset. The light blue trace is the PV dataset and the white represents the output experienced at the POI. The violet trace in the lower chart illustrates the actual BIS output.

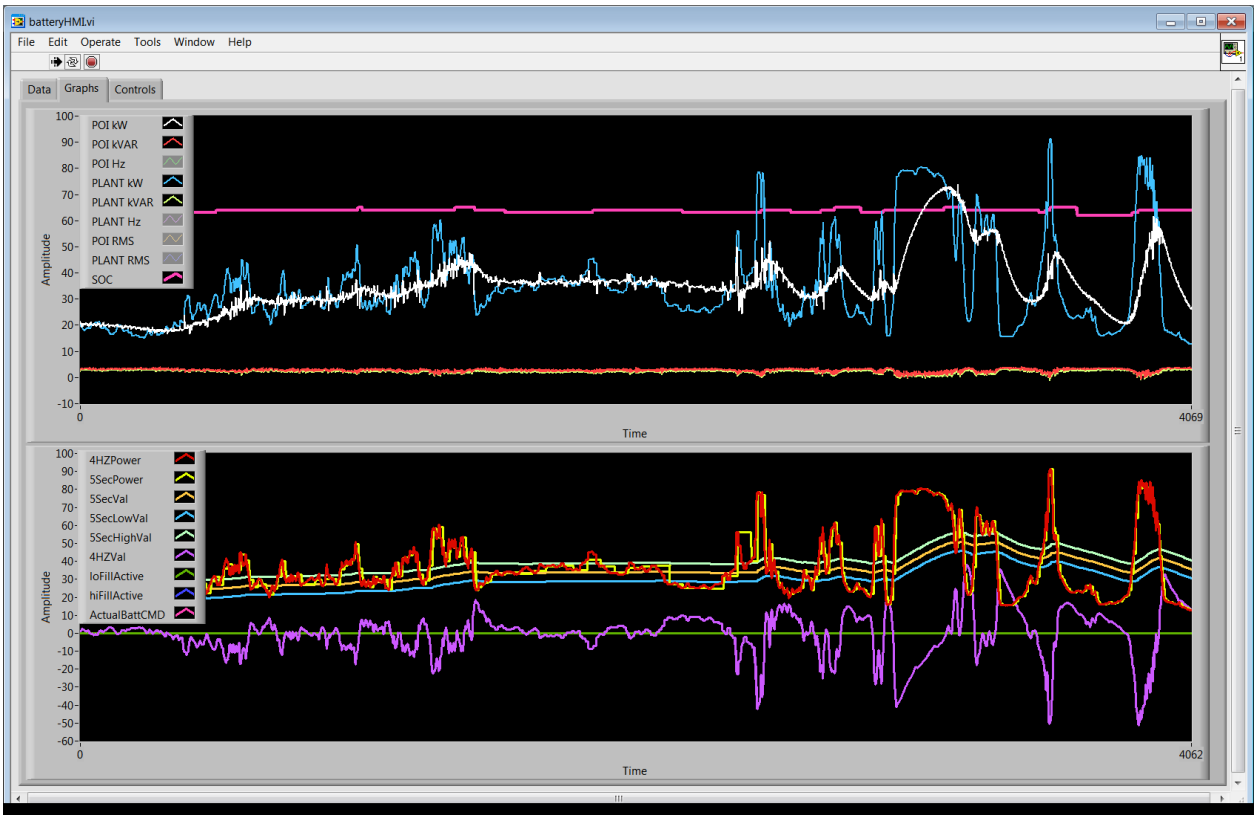

Figure 29: Ramp controller HMI illustrating PV, storage system, and POI energy flows as well as debugging variables

Other developments:

Excursion limiting: In the course of developing the smoothing control algorithms and researching storage needs, the team came up with a novel approach to further 'firming' the DER resource. This approach was coined excursion limiting and is an overlay of the smoothing functionality with a secondary control algorithm that has the net effect of significantly limiting the power excursions in both the upward and downward direction effectively shifting the peaks to the valleys and vice-versa enabling a much firmer power profile that can be depended upon by electricity operators. This application could be added to the overall suite of storage inverter system functions. Since the energy capacity of the battery far exceeds the requirement for ramping (due to the power need and C rate limitations of the battery), this capacity could be used to further firm the PV output, or be used for other applications like peak shifting. For this reason, the team also elected not to focus on state of charge management, as it was deemed a higher level function that would be managed likely by the utility or some form of energy management controller.

Economics: Significant progress was not made in this area during the program period. However, a quick look at the Baldock site economics highlights the reality that storage

technology prices must continue to decline to make storage broadly viable for utility scale smoothing applications. Implementing the 300kW BIS and ramp controls at the Baldock site would add roughly 20-30% additional cost to this site. Noteworthy also that this particular installation required far less battery than expected and less than many installations would require, so it could be estimated storage might add as much as 50% to the cost of a PV installation. This would cause developers to look for another site where ramp controls are not needed – eventually as penetration levels increase and storage prices decline, a cross-over point will be met.

Future work

As mentioned earlier in the report the utility partner and site for this demonstration (PGE/Baldock 1.4MW PV site) made business decisions in year three of the program that made actual installation of the storage system on their grid impossible. The team identified a new partner to site the storage system, but there was not sufficient time remaining in the program to get the system sited and operational. Additionally the 300kW/300kWh Saft battery and AE500TX storage inverter are interconnected and cycling the battery at the AE facility, but final integration of the PMU's and cRIO controller was not completed at the conclusion of the SEGIS program. Full testing was performed on the 50kW scale battery and inverter, but the team plans to repeat this on the full scale 300kW system before siting the BIS. Further work should be done to make system sizing and validation more efficient to reproduce. And finally, once the specific storage system requirements and application have been defined, the system should go through a rigorous product development initiative to translate the prototype system developed into a reproducible and economical product. Demonstration sub-tasks were not able to be completed at the conclusion of the SEGIS-AC program due to lack of a demonstration site. However, smoothing was demonstrated successfully onsite at the AE site in Bend, OR.

Conclusions

The SEGIS-AC program was successful in meeting the majority of the outlined goals. Some of the stretch goals were not met, but were included given the nature of the program, partnerships, and the evolution of the solar industry. Fundamental successes include significantly improving industry awareness of synchrophasor based islanding detection, as well as ultimately by the end of the program creating "pull" from a host of utilities. Until recently the team was "pushing" awareness of the technique, and recently a transition has occurred where utilities are aware of the emerging need and engaging in practical and business discussions regarding implementation. Smart inverter control functionality is now available in all of Advanced Energy's inverter product lines and the capability has been tested at both Sandia National Laboratories and at NREL. These utility interactive control features were also demonstrated on a live feeder at Portland

General Electric and are in use on various PV plants throughout North America. Additionally, an integrated storage system was developed along with control algorithms and implementation for intermittency mitigation. This program enabled industry advancements that fundamentally would not have been possible in the three year time frame and has laid a strong foundation for continued integration onto the utility grid. This coupled with the steep decline in the installed cost of PV systems is bringing solar to the mainstream.

Budget and Schedule

There were several revisions to the program budget and SOPO over the period of performance. These revisions resulted from ongoing refinement to the scope and objectives of the program and ultimately the divergent interests between AE and the prime utility partner. The largest variance resulted in BP3 when siting and commissioning of the battery-inverter system became unfeasible. There were significant funds reserved for travel (54% variance) and supplies (46% variance) in support of system setup, commissioning, test and demonstration. Significant variance in the contractual category (47%) is attributed to not following through with site preparation, excavation, concrete work and transportation logistics. The cost of the SAFT 300kWH battery ($464,666) was included in the program budget but the decision was made to capitalize the expense instead so the expense never hit the program.

NPPT played a larger role (143% variance) in contributing to the program deliverables than the approved budget initially accounted for. This is attributed to the loss of key personnel from AE requiring NPPT to increase their scope of work to fill in the gaps.

The program completed on time (April 30, 2015) and under budget ($5.26M budgeted, $2.98M spent)

Table 11 Advanced Energy SEGIS-AC program spending summary

Recipient:	**Advanced Energy**
DOE Award #:	**DE-EE0005340**

Spending Summary by Budget Category						
	Approved Budget per SF-424A				**Actual Expenses**	
Budget Categories per SF-424a	**BP 1**	**BP 2**	**BP 3**	**Total**	**Cumulative**	**%**
a. Personnel	$367,661	$273,087	$194,050	$834,798	$783,003	93.80%
b. Fringe Benefits	$93,754	$69,637	$49,483	$212,874	$199,666	93.80%
c. Travel	$35,500	$27,500	$27,500	$90,500	$49,079	54.23%
d. Equipment	$150,000	$337,500	$187,500	$675,000	$194,604	28.83%
e. Supplies	$271,534	$186,930	$29,123	$487,587	$224,195	45.98%

f. Contractual	$519,776	$847,603	$441,410	$1,808,789	$853,944	47.21%
g. Construction	$0	$0	$0	$0	$0	0.00%
h. Other	$0	$0	$79,874	$79,874	$45,594	57.08%
i. Total Direct Charges	**$1,438,225**	**$1,742,257**	**$1,008,940**	**$4,189,422**	**$2,350,085**	**56.10%**
j. Indirect Charges	$396,564	$443,260	$229,772	**$1,069,596**	$630,400	58.94%
k. Total Charges	**$1,834,789**	**$2,185,517**	**$1,238,711**	**$5,259,018**	**$2,980,485**	**56.67%**
DOE Share				$3,100,000	$1,738,514	56.08%
NPPT Share				$226,776	$325,366	143.47%
AE Cost Share				$1,932,242	$908,018	46.99%
Non-Gov Cost Share Percentage	0.0%	0.0%	0.0%	41.1%	41.4%	100.80%

Path Forward

For the CCB island detection algorithm, the next step is large-scale field demonstrations and trials. The Advanced Energy team is working closely with a number of utility partners to identify sites for this work. This should be considered a significant success of the SEGIS-AC program: the CCB is essentially ready for beta testing and will move into that phase in the next twelve months.

Regarding the advanced inverter control functions, the market for these is likely to significantly increase within the next year or two. California Rule 21 is requiring inverters to have these capabilities in the near term (not necessarily to have the functions *active*, but the *capability* must be there to enable future activation), and as of this writing, Hawaii is following the Rule 21 example but is likely to require smart inverter function implementation even sooner than California due to their PV penetration levels. Interest in smart inverter functions is also growing on the east coast, and it seems likely that several eastern US utilities or ISOs will adopt smart inverter requirements in CY 2015.

Regarding the BIS, the team is finalizing development of the prototype and actively engaged in discussions with an interested utility partner regarding siting of the system that will ultimately result in demonstration and further development and optimization. While storage for utility integration remains cost prohibitive in most cases, utilities are beginning to look at storage systems to mitigate transients, delay or eliminate the need for line extensions, and other areas. Utility scale storage is getting written into the five year plan for many utilities. Storage will continue to become more relevant as storage technology costs decrease and low cost low penetration PV sites become more scarce.

References

References are noted as used in the footnotes of the document.